ELEMENTA
Science of the Anthropocene

RESEARCH ARTICLE

Weakened pelagic–benthic coupling on an Arctic outflow shelf (Northeast Greenland) suggested by benthic ecosystem changes

Yasemin V. Bodur[1,2,*] , Paul E. Renaud[3], Lidia Lins[4], Luana Da Costa Monteiro[4], William G. Ambrose Jr.[5], Janine Felden[6], Thomas Krumpen[7], Frank Wenzhöfer[1,8], Maria Włodarska-Kowalczuk[9], and Ulrike Braeckman[4]

Arctic marine ecosystems are becoming more boreal due to climate change. Predictions of ecosystem change focus mainly on Arctic inflow or interior shelves, with few comprehensive studies on Arctic outflow regions. During September–October 2017, soft-bottom communities were sampled and benthic ecosystem processes were quantified at 12 stations on the Northeast Greenland shelf (outflow shelf) and compared to the last regional ecosystem study, conducted in 1992 and 1993. The benthic habitat was characterized in terms of sediment granulometry, pigment concentrations, and porewater chemistry (dissolved inorganic carbon, nutrients). Total abundance and biomass of macrobenthos and meiobenthos, bacterial abundance, porewater dissolved inorganic carbon and ammonium concentrations were higher on the outer shelf compared to locations adjacent to the Nioghalvfjerdsfjorden glacier at 79°N and the inner shelf stations (e.g., macrofauna: 1,964–2,952 vs. 18–1,381 individuals m^{-2}). These results suggest higher benthic production in the outer parts of the NEG shelf. This difference was also pronounced in macrobenthic and meiobenthic community structure, which was driven mainly by food availability (pigments with 1.3–4.3 vs. 0.3–0.9 µg g^{-1} sediment, higher total organic carbon content and bacterial abundance). Compared to the early 1990s, warmer bottom water temperatures, increased number of sea-ice-free days and lower sediment pigment concentrations in 2017 were accompanied by decreased polychaete and increased nematode abundance and diversity, and a different community structure of nematode genera. The present study confirms previous reports of strong pelagic-benthic coupling on the NEG shelf, but highlights a possible weakening since the early 1990s, with a potential shift in importance from macrofauna to meiofauna in the benthic community. Increasing inflow of Atlantic water and decreasing volume transport and thickness of sea ice through the Fram Strait, probably affecting the Northeast Water Polynya, may be responsible, suggesting ecosystem-wide consequences of continued changes in sea-ice patterns on Arctic shelves.

[1] Max Planck Institute for Marine Microbiology, Bremen, Germany

[2] Department of Arctic and Marine Biology, UiT—The Arctic University of Norway, Tromsø, Norway

[3] Akvaplan-niva, Tromsø, Norway

[4] Marine Biology Research Group, Ghent University, Ghent, Belgium

[5] Coastal Carolina University, Conway, SC, USA

[6] MARUM, Center for Marine Environmental Sciences, University Bremen, Bremen, Germany

[7] Alfred Wegener Institute Helmholtz Centre for Polar and Marine Research, Sea Ice Physics, Bremerhaven, Germany

[8] HGF-MPG Group for Deep Sea Ecology and Technology, Alfred Wegener Institute Helmholtz Centre for Polar and Marine Research, Bremerhaven, Germany

[9] Department of Marine Ecology, Institute of Oceanology, Polish Academy of Sciences, Sopot, Poland

*Corresponding author:
Email: yasemin.bodur@uit.no

1. Introduction

The marine environment in the Arctic is characterized by the high seasonality of the solar cycle and sea-ice dynamics, which in turn determine the dynamics of nutrient availability and primary production and with that, the availability of food in the ecosystem. Pathways of secondary production in high latitude ecosystems depend on the match of timing between this seasonal primary production and pelagic consumer development (Sakshaug et al., 2009; Meire et al., 2016). Pelagic mineralization patterns determine the amount of organic matter (OM) that ultimately sinks to the seafloor and serves as food for benthic communities (Graf, 1989; Jensen et al., 1990; Wassmann and Reigstad, 2011; Wiedmann et al., 2020). A strong dependency of benthic ecosystems on pelagic-benthic coupling in the Arctic has been documented for fjord (McMahon et al., 2006) and shelf systems (Grebmeier

et al., 1988; Ambrose and Renaud, 1995; Carmack and Wassmann, 2006; Renaud et al., 2008), as well as for the deep Arctic Ocean (Degen et al., 2015; Wiedmann et al., 2020).

The vertical export of OM in the Arctic Ocean varies regionally, with marginal ice zones and polynyas regarded as particularly productive sites (Spies, 1987; Sakshaug and Skjoldal, 1989; Niebauer et al., 1990; Piepenburg, 2005; Grebmeier and Barry, 2007; Wassmann and Reigstad, 2011). Pelagic variations in primary production are usually reflected in the availability of OM at the seafloor and determine the variability of benthic communities (Piepenburg et al., 1997; Bourgeois et al., 2016). Pelagic processes, both physical (e.g., lateral advection) and biological (zooplankton grazing, microbial recycling), influence the pelagic export (Grebmeier and Barry, 1991), with significant impacts on the functioning of underlying benthic communities (Morata et al., 2015).

Changing sea-ice dynamics in the Arctic are expected to have significant consequences for the composition and timing of OM production, with potential impacts on the quality and quantity of food reaching the benthos (Piepenburg, 2005; Carmack and Wassmann, 2006; Wassmann and Reigstad, 2011; Smith et al., 2013; Mäkelä et al., 2017; Hoffmann et al., 2018), and on the fate of the OM at the seafloor (Braeckman et al., 2018). The Arctic sea-ice extent is declining at an accelerating rate (Overland and Wang, 2013; Comiso et al., 2017; Onarheim et al., 2018; Meredith et al., 2019), resulting in an expansion of openwater areas across the Arctic (Overland and Wang, 2013; Barnhart et al., 2016; Comiso et al., 2017; Onarheim et al., 2018). Accordingly, the export of sea ice through Fram Strait, as well as the sea-ice thickness off Northern Greenland, have declined significantly during the last two decades (Spreen et al., 2020; Sumata et al., 2022). Moreover, the heat transport toward the high North through warming water masses (Spielhagen et al., 2011; Beszczynska-Möller et al., 2012; Polyakov et al., 2020; Skagseth et al., 2020; Smedsrud et al., 2022) and enhanced glacial melt, especially from Greenland's glaciers (Rignot and Kanagaratnam, 2006; Nick et al., 2013), are further effects that coincide with climate change. Alterations in ocean temperature and sea-ice cover will also affect the dynamics of seasonal ice zones and polynyas (April et al., 2019), which are hotspots of the food supply for benthic communities (Grebmeier and Barry, 2007), and most likely lead to drastic changes in Arctic ecosystems through all trophic levels (Wassmann et al., 2011).

A longer period of light availability through reduced sea-ice cover might fuel phytoplankton blooms (Arrigo et al., 2008), but the establishment of a bloom and the export of OM depends on multiple factors such as nutrient availability and vertical mixing, induced for example by wind stress (Ardyna et al., 2014). Despite an overall increase in primary production by 30% in the Arctic during the course of the last two decades, primary production on outflow shelves has either decreased or shown no change (Arrigo and van Dijken, 2015). An efficient transport of OM to the seafloor will most likely be influenced by whether locally changing sea-ice dynamics will favor a stratified or mixed regime in the water column (von

Appen et al., 2021). Moreover, sea-ice algae can contribute substantially to total primary production (Horner and Schrader, 1982; Hegseth, 1998) and are regarded as a food source with higher nutritional value (Falk-Petersen et al., 1998; McMahon et al., 2006).

During the first biological observations in the early 1990s, a tight pelagic-benthic coupling was reported for the Northeast Greenland (NEG) shelf, especially within the Northeast Water (NEW) Polynya, located on the northern part of the shelf (Ambrose and Renaud, 1995; Hobson et al., 1995; Piepenburg et al., 1997; Rowe et al., 1997). Within the NEW Polynya, higher primary production and/or reduced pelagic mineralization resulted in higher benthic production compared to the ice-covered southern part of the NEG shelf (Ambrose and Renaud, 1995; Stirling, 1997). Benthic communities were strongly associated with OM input from the pelagic realm (Piepenburg et al., 1997), and thick ice algal aggregates potentially served as a rich energy source (Gutt, 1995; Bauerfeind et al., 1997). Since these findings, no further biological studies have been carried out in this region. At that time, the Norske Øer Ice Barrier (NØIB) in front of Nioghalvfjerdsfjorden (79°N Glacier), hindered investigations on benthic communities near the glacier.

Today, glacial melt, increasing sea-ice melt and thinning, as well as stronger input of warm Atlantic Water, are acting in concert in altering the NEG shelf between 77°N and 81°N. Since 2003, glaciers around NEG have undergone sustained thinning, and the seasonal floating tongue of the 79°N Glacier, the largest marine-terminating glacier on the NEG shelf, retreated by more than 100 m yr^{-1} between 2001 and 2011 (Khan et al., 2014). Increasing temperatures have led to seasonal break-up events of the NØIB fast ice cover, which historically broke up only in intervals of several decades (Reeh et al., 2001). The NØIB not only stabilizes the floating glacier tongue and constrains its melting, but also blocks advection of sea ice into the NEW Polynya region. As a result, the NEW Polynya, which has been recurring seasonally for at least 1,000 years (Syring et al., 2020), has become a less obvious phenomenon in the last decade: the patterns in sea-ice cover have become much more dynamic, with a more extensive open water area (Reeh et al., 2001; Smith and Barber, 2007; International Space Science Institute [ISSI], 2008; Reeh, 2017). Moreover, NEG receives a substantial amount of freshwater from the southward sea ice and from freshwater transport through Fram Strait, which, together with glacial meltwater, has already led to a substantial freshening of the coastal subsurface waters in this area (Sejr et al., 2017). Therefore, the NEG outflow shelf is especially susceptible to stratification (Carmack and Wassmann, 2006). Additionally, there is an increasing influence of warm Atlantic Water on the shelf (Schaffer et al., 2017).

For the first time since 1993, a reassessment of the spatial patterns of benthic communities and their ecosystem functions was carried out on the NEG shelf during a field campaign in 2017. To investigate their response to ongoing glacial melt, sea-ice thinning and stronger input of Atlantic Water, we compared environmental conditions,

benthic oxygen uptake and remineralization processes, and benthic community parameters (abundance of macrofauna, meiofauna, and bacteria, and macrofaunal and meiofaunal biomass and community composition) with patterns described in 1992 and 1993 during investigations carried out with USCGC *Polar Sea* and R/V *Polarstern*. We hypothesized that increasing stratification and the disappearance of the NEW Polynya resulted in a decoupling of the benthos from the pelagic environment with decreased OM supply to the seafloor, and consequently reduced abundances and functions of benthic communities on the NEG outflow shelf.

2. Materials and methods
2.1. Study site
The NEG continental shelf extends more than 300 km from the coastline (**Figure 1**). Between 77°N and 81°N, two troughs are present: the Westwind Trough in the north and the Norske Trough in the south, which together half-encircle shallow banks of water depths <200 m located approximately in the middle of the shelf (Arndt et al., 2015; Schaffer et al., 2017). The bathymetry of the trough system provides a valley between the shelf break of the Norske Trough in the south and the shelf break of the Westwind Trough in the north, allowing warm and saline Atlantic Intermediate Water (AIW) originating from the recirculation into the East Greenland Current to enter the NEG shelf via the Norske Trough (Schaffer et al., 2017). AIW occupies depths below 150–200 m (subsurface AIW) and circulates in an anticyclonic way across the shelf (Bourke et al., 1987).

As part of the Northeast Greenland Ice Shelf, the 79°N Glacier has a large floating ice tongue that fills the entire interior of the 79°N Fjord (Thomsen et al., 1997). Underneath is a trough with a maximum depth of more than 900 m, where subglacial melting takes place with a mean melt rate as fast as 8 m yr^{-1} (Mayer et al., 2000). Water warmer than 1°C below the 79°N Glacier (Wilson and
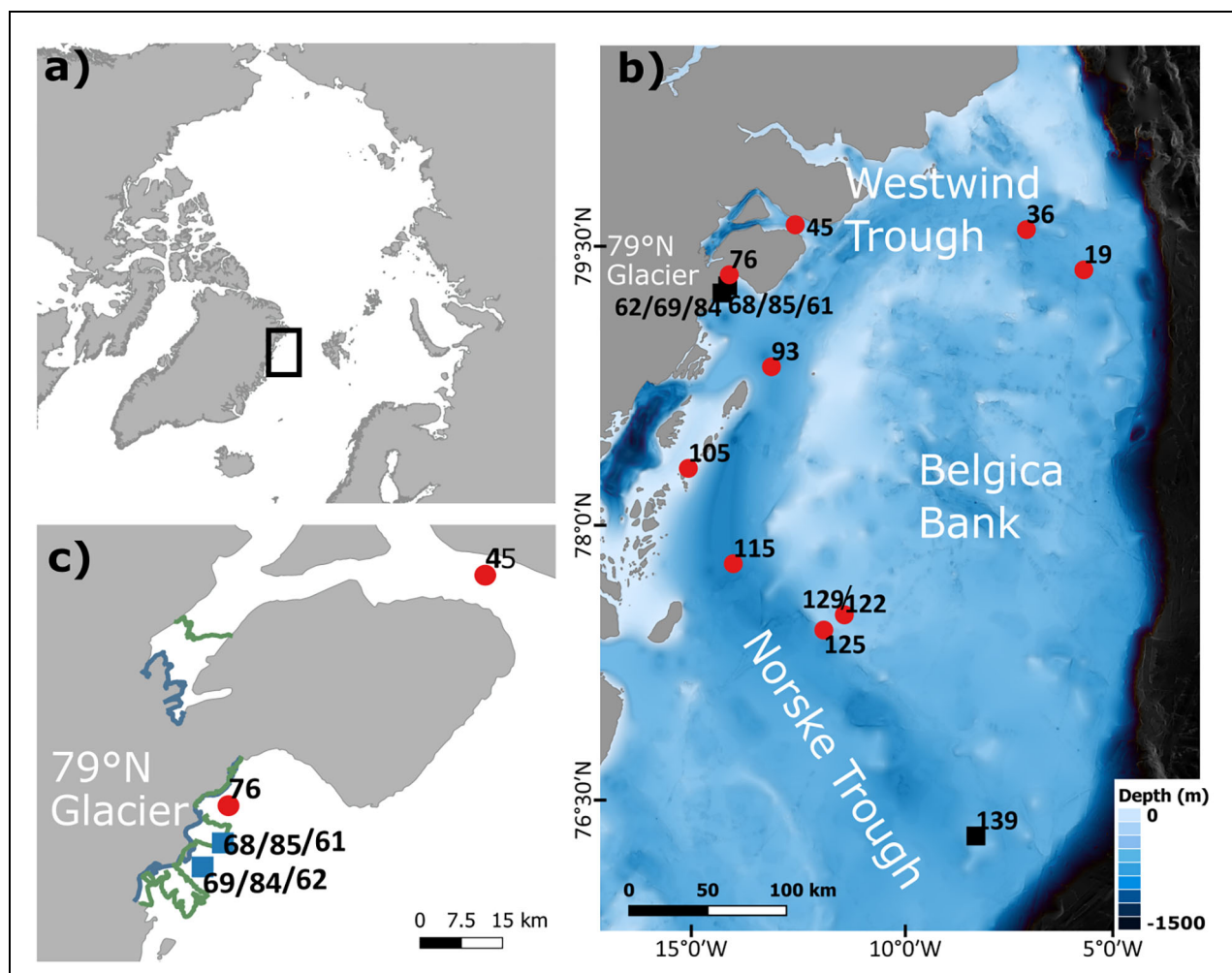

Figure 1. Sampling locations on the Northeast Greenland shelf during 2017. (a) Overview map showing the location of the study area in the Arctic. (b) Station locations from the R/V *Polarstern* cruise PS109 in 2017. Red dots indicate multicorer stations and black rectangles indicate stations where a benthic lander was also used. (c) Closeup of the Glacier stations with calving front from 1990 (green) and 2017 (blue). Background bathymetry is based on the International Bathymetric Chart of the Arctic Ocean (Jakobsson et al., 2020), Coastlines were obtained from Wessel and Smith (1996). Calving front data from 1990 (green line) and 2016 (blue line) were retrieved from the Environmental Earth Observation IT GmbH (ENVEO, 2017).

Straneo, 2015) causes basal melting in this cavity (Mayer et al., 2000; Straneo et al., 2012; Schaffer et al., 2017). Modified AIW leaves the glacier cavity through the calving front and through the Djmphna Sund (Schaffer, 2017), which is located north of the glacier front. The AIW throughout the whole trough system has warmed. In the period between 1979–1999 and 2000–2016, the Norske Trough experienced a temperature increase of 0.5°C (Schaffer et al., 2017; Mayer et al., 2018; Schaffer et al., 2020).

At around 79°30'N, the NØIB, a semi-permanent land-fast sea-ice cover and at one time one of the largest areas of landfast ice on Earth (Hughes et al., 2011), was observed to hinder the advection of sea ice into the NEW Polynya at its southern extent (Minnett et al., 1997). The polynya used to open in April or May and close around September (Schneider and Budéus, 1994). It varied in size, located around 80°N in the Westwind Trough, and was reported occasionally to cover an area of 44,000 km^2 (Wadhams, 1981). Two break-ups of the NØIB were observed until 2001, namely in the 1950s and in 1997, which led to an extended open-water area and enhanced calving of the 79°N Glacier (Reeh et al., 2001). Between 2002 and 2005, the NØIB broke up every summer (Hughes et al., 2011).

2.2. Sampling and laboratory analyses

Samples were taken in September and October 2017 during cruise PS109 of the R/V *Polarstern* at 17 multiple corer (MUC) and lander stations at water depths between 140 m and 645 m. Because different deployments of instruments at the same aimed position received individual station numbers, some stations were pooled (namely 69/84/62, 68/85/61, and 122/129), resulting in 12 locations that are henceforth referred to as "stations" (**Figure 1b**, Table S1). Three stations were located in the Westwind Trough, 5 stations in the Norske Trough, and 3 stations close to the 79°N Glacier (Table S1). One station (locations 122 and 129) was located on the shallow Belgica Bank (water depths of 140 m and 139 m, respectively). At each station, a camera-equipped MUC (TV-MUC; core area of 0.007 m^2) was deployed to collect sediment cores for ex situ measurements of oxygen consumption and sediment sampling. Additional in situ oxygen flux measurements were performed with an autonomous benthic lander at three of these stations, one at the outer Norske Trough (Station 139) and two at the margin of the 79°N Glacier (Stations 68 and 69; Table S1). In the following, lander stations are denoted with the suffix "-L" to distinguish them from MUC stations.

CTD profiles (Kanzow et al., 2018) for each benthic station were obtained for temperature and salinity. When a CTD profile was not taken directly at the benthic station, the data from the CTD closest to the station was used (maximum distance to the nearest CTD was 31.5 km at Station 139). At Station 68/85/61, the closest CTD (distance of 13 km) was at a location with a depth of 400 m, so the data from 150 m depth, which was the depth of the benthic station, was taken as bottom water. Bottom water temperatures ranged between −1.07°C and 1.76°C and salinities between 33.96 and 34.94.

2.2.1. Sediment solid–phase parameters

Upon arrival on deck, the upper 5 cm of three MUC cores were sampled in 1 cm intervals with 5 mL cut-off syringes for granulometry, porosity, benthic pigments (chlorophyll *a* (Chl *a*), phaeopigments and fucoxanthin), total organic carbon (TOC), and total nitrogen (TN). Because these cores originated from the same deployment, they are technically pseudoreplicates. Time constraints, however, did not allow for truly replicated deployments. For granulometry, the sediment was sliced in 1 cm intervals and stored in 20 mL scintillation vials or plastic bags. Grain size spectra were assessed by laser diffraction (Malvern Instruments, Malvern, UK; Braeckman, 2023a). Porosity samples were stored in 5 mL cut-off syringes wrapped in aluminum foil. In the laboratory, the samples were sliced in 1 cm sediment depth intervals and the wet mass of the sediment samples was measured and then dried at 60°C in a drying oven. Porosity was calculated by the difference between the wet and dry mass of the samples after Dalsgaard et al. (2000; Braeckman, 2023b).

Chl *a*, phaeopigments (phaeophorbide *a* and phaeophytin *a*) and fucoxanthin were subsampled with 10 mL cut-off syringes, which were pushed gently into the sediment until reaching 5 cm depth, and stored at −80°C. In the laboratory, the samples were sliced in 1 cm horizons and analyzed using high performance liquid chromatography after Wright and Jeffrey (1997; Braeckman, 2023c). Quantities are expressed as microgram pigment per gram of dry sediment (μg g^{-1}). The chloroplastic pigment equivalent (CPE) was calculated as the sum of Chl *a* and phaeopigments.

TOC and TN were determined by treating an aliquot of dried sample with hydrochloric acid until no more bubbles were observed, to remove inorganic carbon prior to analysis. Percent TOC and TN were determined in sediments dried at 250°C using a ELTRA CS2000 Carbon Analyzer (Braeckman, 2023d).

For comparison with the earlier studies, CPE and TOC were converted to grams per meter squared using porosity and sediment density (2.55 g cm^{-3}) in the following equation:

$$\frac{\mu \, g \text{ CPE or TOC}}{g \text{ (dry sediment)}} \times (1 - \text{porosity}) \times \text{density} \times 1 \text{ cm} \times 10,000$$

2.2.2. Sediment porewater parameters

At each station, two MUC cores with pre-drilled holes were mounted on the MUC for porewater extractions. Samples for measuring porewater chemistry (DIC, nutrients, sulfate and sulfide concentrations) were collected with Rhizon samplers (pore size 0.2 μm, Rhizosphere, Wageningen, Netherlands) by inserting them carefully into the pre-drilled holes on the retrieved MUC cores with depth intervals of 1 cm until 10 cm sediment depth, and 2 cm intervals until 20 cm sediment depth. The porewater of the two MUC cores was pooled; a total of 9 mL porewater for each depth interval was retrieved in this manner.

To determine the concentration of dissolved inorganic carbon (DIC), 2 mL porewater was sampled in glass vials pre-treated with HgCl$_2$ and stored at 4°C. DIC

concentrations were measured using a flow injection system equipped with the Spark Optimas auto-sampler (model 820, Ambacht, Netherlands). For the analysis of porewater nutrients, 4 mL of porewater was transferred to acid-washed Sarstedt Vials, stored at $-20°C$ and further subsampled in the home lab before analysis (4 mL for phosphate, silicate and ammonium, 1 mL for nitrate and nitrite). Samples were analysed with a Continuous Segmented Flow Analyser (QuAAtro39, SEAL Analytical; Braeckman and Felden, 2023).

2.2.3. Sediment oxygen profiles and oxygen fluxes at the sediment–water interface

For the assessment of ex situ fluxes at the sediment-water interface, part of the overlying water from three cores was removed and stored at in situ temperature separately, while the height of the remaining water above the sediment was adjusted to 10 cm by gently pushing the sediment vertically upwards without disturbing the surface sediment layer. The cores were transferred to a temperature-controlled water bath where the temperature had been adjusted to the in situ values in the bottom water at the respective station (information retrieved from shipboard sensors). The overlying water was homogenized with a magnetic stirrer, and the water surface was gently streamed with a soft air stream to aerate the overlying water.

For the quantification of diffusive oxygen uptake (DOU), two oxygen microprofiles were measured simultaneously, ideally within 2 h of sampling (in some cases >24 h, namely Stations 139, 85, 84, and 76) and for each sediment core with 2 oxygen optodes (Pyroscience, Firesting; tip size 50 µm) mounted on an autonomous microprofiler module. The sensors were two-point calibrated using on-board signals recorded in air-saturated surface seawater and anoxic, dithionite-spiked bottom water at in situ temperature (Felden et al., 2023).

After microprofiling, total oxygen uptake (TOU) was assessed from the decrease in oxygen concentration in the overlying water over time for approximately 48 h (at least 36 h). The cores were closed with no air bubbles in the overlying water, and magnetic stirrers ensured the homogenization of the overlying water. An oxygen optode (Pyroscience, Firesting) measured the oxygen concentration continuously in the overlying water (measuring interval of 60 s, calibrated as described above). Total sediment oxygen flux was determined as the decrease in oxygen concentration in the water phase, which was read from the continuous oxygen sensor data. The incubation was terminated at $\leq80\%$ initial $[O_2]$ (Braeckman and Wenzhöfer, 2023).

To quantify in situ fluxes at the sediment-water interface, an autonomous benthic lander equipped with three benthic chambers (area of 0.04 m^2), a sediment profiler and a Niskin bottle were deployed at selected stations. Upon arrival at the seafloor and a waiting time of 4 h after the lander deployment to allow resuspended matter to settle (Glud et al., 1994; Tengberg et al., 1995; Donis et al., 2016), the lander chambers were driven slowly into the sediment. The lander chambers enclosed 20 × 20 cm of sediment and about 10–15 cm of overlying water

(depending on the final orientation of the lander). The enclosed overlying water was gently stirred to avoid stagnation. A syringe sampler collected overlying water samples at regular times for the analysis of nutrients and DIC, while an Aanderaa optode (4330, Aanderaa Instruments, Norway, two-point calibrated as described above) continuously measured the oxygen concentration in the overlying water every 10 min during the total incubation time of around 48 h.

At the end of the incubation, chambers were closed and the incubated sediment was retrieved with the lander from the seafloor. On board, the volume of overlying water in the chambers was estimated from the surface and the height of the overlying water body, measured with a ruler at 6 to 8 positions within each chamber and subsampled for the above-mentioned sediment parameters.

Simultaneously to the chamber incubations, electrochemical oxygen microsensors (adapted and customized after Revsbech, 1989, and calibrated with a two-point calibration) measured in situ oxygen profiles at 3–5 points. The bottom water oxygen concentration (taken from the Niskin bottle and estimated by Winkler titration) was used as the first calibration point. When the sensor had reached the anoxic zone of the sediment, the sensor signal at this point was taken as the second calibration point. Otherwise, the sensor signal in an anoxic solution of sodium dithionite was used. The maximum profiling depth of the profiler during in situ measurement was 180 mm, with profiling resolution of 100 µm.

Both ex situ (MUC cores) and in situ (lander) DOU fluxes across the sediment-water interface were calculated from running average-smoothed oxygen profiles using Fick's first law (Glud et al., 1994). Ex situ TOU fluxes were calculated from the initial linear decrease in O_2 concentration versus time (first 30 h) in the enclosed overlying water body (Glud et al., 1994). Due to issues with optodes, in situ TOU fluxes could only be measured at Station 139-L.

2.3. Benthic community parameters
2.3.1. Bacterial abundance
The upper 5 cm of the sediment was sampled with a 10 mL cut-off syringe and sliced into 1 cm layers, corresponding to 2 mL marked on the syringe. Each slice was transferred to a scintillation vial, and fixed by adding 9 mL of filtered (0.22 µm) 3% (final concentration) formaldehyde-artificial seawater solution. Afterwards, the samples were diluted further with the same solution, filtered through polycarbonate filters (0.2 µm, Whatman Nuclepore Track-Etch Membrane) and stained with a 0.001% acridine orange solution after Hobbie et al. (1977). Single cell abundances were estimated from counts of at least 30 grids for 2 replicate filters per sample with a Zeiss Axiophot microscope (Germany) and a 100× oil immersion objective lens (Zeiss Plan-Apochromat, Germany; Bodur et al., 2023a). For each 1 cm layer, quantities are expressed in cells mL^{-1} (equivalent to 1 cc wet sediment) after accounting for all dilution steps. For summed layers, 0–5 cm, used as an environmental variable (Section 2.5.1), quantities are expressed in cells cm^{-2}.

2.3.2. Macrofaunal and meiofaunal communities

At the end of the ex situ incubations, the MUC cores were opened and meiofaunal communities were sampled with a cut-off 10 mL syringe (area 1.89 cm^2) to 5 cm sediment depth. This subsample was further sliced in 5 horizons of 1 cm. The leftover sediment in the MUC core was sliced into 0–5 cm and 5–10 cm layers and sieved over a 500 µm mesh to collect macrofauna. Sediments from lander chambers were sieved entirely on a 500 µm mesh. Samples were stored in 4% seawater-buffered formaldehyde in Kautex bottles at room temperature.

In the lab, the samples were stained with Rose Bengal. Macrofaunal individuals were identified to the lowest possible taxon level. The blotted wet formalin weight of macrofaunal individuals was determined with a DeltaRange XP56 or AX205 precision balance (Mettler Toledo, Ohio, USA), depending on the organism size and weight. It should be noted that, because of the extremely small size of some specimens, the evaporation of water led to a steady decrease of weight on the precision balance. Polychaetes were removed from their tubes before weighing, and molluscs were weighed with their shells. Other encrusting and calcifying organisms such as bryozoans were also weighed with their tests, such that their biomass is most likely overestimated. Colonial animals such as Bryozoa and Hydrozoa were weighed for biomass estimations but excluded for density and community analysis. When no head was present in the sample but body segments were, polychaete taxa were counted as one specimen due to the general low abundance of specimens in the samples. Nematoda and other worms that inhabited foraminifera tests (Nematoda, small Nemertea) were excluded from the biomass and density calculations as they were not part of the macrofaunal communities (Bodur et al., 2023b).

For the representation of total biomass, the wet weight of individuals >1,000 mg was removed in order to reduce skewing of the data: 1 individual of *Ctenodiscus crispatus* (5,773 mg, Station 139), *Ophiopleura borealis* (3,048 mg, Station 68), *Allantactis parasitica* (3,018 mg, Station 139), *Priapulus bicaudatus* (2,846 mg, Station 36), and *Ophiocten sericeum* (1,471 mg, Station 129). All other individuals were <712 mg. We preferred removing these outliers instead of transforming the data.

Samples from the 5–10 cm sediment depth from the stations with the highest faunal abundance (Stations 36, 125, and 129) were checked for presence of fauna. Only one body part of a specimen of Maldanidae was found in one sample from Station 36; therefore, sediment depths >5 cm were not considered further for community analyses.

Meiofauna were extracted from the samples by triple density centrifugation with the colloidal silica polymer LUDOX TM 40 (Heip et al., 1985) and rinsed with freshwater on stacked 1 mm and 32 µm mesh sieves. The fraction retained on the 32 µm mesh sieve was preserved in 4% Li$_2$CO$_3$-buffered formalin and stained with Rose Bengal. All metazoan meiobenthic organisms were classified at higher taxonomic levels and counted under a stereoscopic microscope (Leica MZ 8, 16×5×; Da Costa

Monteiro et al., 2023a). All Nematodes of each sample were handpicked with a fine needle, transferred to glycerine (De Grisse I, II, and III; Seinhorst, 1959), mounted on glass slides, identified to genus level based on the Nemys website (Nemys, 2022), and allocated to functional feeding groups based on Wieser (1953) as selective deposit feeders (1A), non-selective deposit feeders (1B), epistratum feeders (2A) or predators/scavengers (2B; Da Costa Monteiro et al., 2023b).

2.4. Data utilized from 1992 and 1993

Data from the early 1990s for bottom water temperature, sediment CPE, TOC content, TOU and Polychaeta and Nematoda abundances were available from campaigns of the US Coast Guard vessel *Polar Sea* between July 18 and August 1, 1992, and from R/V *Polarstern* during cruises PS25 and PS26 between May and August 1993 (Ambrose and Renaud, 1995; Piepenburg et al., 1997; Rowe et al., 1997; Renaud and Ambrose, 2023). A map of the stations from 1992 and 1993 that were used for comparison is given in **Figure 2**. For TOC and CPE content, one subcore (1.9 × 2 cm) from 2–7 replicate boxcores (0.25 m^2) was taken at each station. Three subcores (8 × 15 cm) sampled from each boxcore were taken for Polychaeta and subsequently sieved through 500 µm mesh sieve. For further details see Ambrose and Renaud (1995) and Renaud and Ambrose (2023). Nematodes were sampled with a multi-corer, from which one subsample of 50 mL sediment was taken (16.67 cm^2 down to 3 cm depth; see Piepenburg et al., 1997; Preben and Herman, 2023). Benthic respiration was measured in situ by deploying benthic chambers, as well as ex situ with shipboard micro-incubation chambers (Rowe et al., 1997).

2.5. Data processing and statistical analyses

2.5.1. Analysis of benthic environmental and community patterns from 2017

For data analysis, the number of sea-ice-free days within the sampling year was calculated for each of the stations rather than selecting a daily resolution of sea-ice concentration because processes in the upper water column are reflected in the benthic communities after a time lag (Rowe et al., 1997). The applied sea-ice concentration product is provided by CERSAT (Ezraty et al., 2007) on a 12.5 km grid and is based on 85 GHz Special Sensor Microwave/Imager brightness temperatures, using the ARTIST Sea Ice algorithm (Kaleschke et al., 2001). Water depth values were taken from the benthic MUC stations. Values for bottom water temperature and salinity were taken from the deepest point measured by the shipboard CTD (Kanzow et al., 2018). For median grain size and silt fraction at each station, the mean value across all sediment depth layers was taken. Pigment concentrations and single cell abundances were integrated (summed) over the top 0–5 cm sediment. Measurements of environmental parameters, single cell abundances, and macrofaunal communities obtained by landers were taken as additional station data replicates, when available.

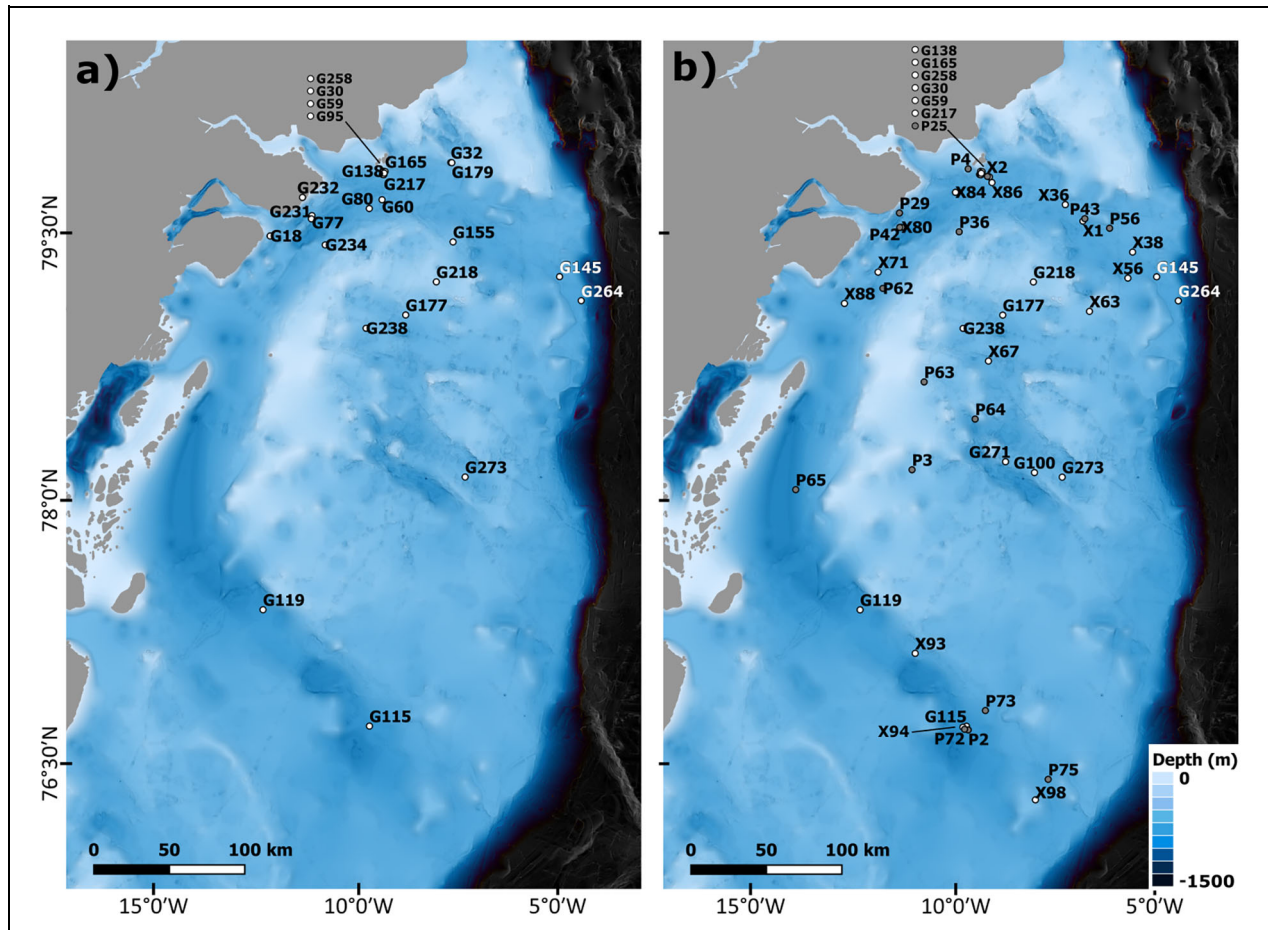A similarity profile routine (SIMPROF) analysis was performed on standardized (scaled to zero mean and unit

Figure 2. Sampling locations during the 1992 and 1993 USCGC *Polar Sea* and R/V *Polarstern* campaigns. Stations sampled for the (a) Nematoda and (b) Polychaeta data used in this study. Locations taken from Ambrose and Renaud (1995), Piepenburg et al. (1997), and Rowe et al. (1997). Sampling years are distinguished by gray (1992) and white (1993) circles.

variance) environmental variables (number of sea-ice-free days, depth, temperature, salinity, grain size, CPE, TOC, TOC/TN ratio, ammonium, DIC, nitrite, phosphate, silicate and single cell abundances) in order to test a priori how many station groups based on the environment were delineated on a significance level of alpha = 0.05. SIMPROF is a cluster analysis tool that determines significant clusters of the stations without a priori grouping of samples. Based on these bias-free results, we divided the communities into the regions distinguished by these significant environmental clusters.

A non-parametric ranked Kruskal–Wallis test was performed on each of the ex situ community parameters (macrofaunal abundance, Polychaeta abundance, macrofaunal biomass, and Polychaeta biomass) in order to test whether the communities at the different stations could be distinguished by environmentally different regions ("sites"; the station clusters formerly delineated by the SIMPROF test based on environmental variables). Kruskal–Wallis was used because no dataset was normally distributed even after transformation and the sample size per group was small.

Two correspondence analyses (CA) were performed on the relative abundances of macrofauna and meiofauna

to visualize the differences in community structure among stations. No transformation was applied to the community datasets. Standardized environmental variables were fitted on top of the species relative abundance ordination to indicate which environmental variables contributed the most to the observed patterns in species abundance.

2.5.2. Comparison with data from the early 1990s

The number of sea-ice-free days within the sampling year at each of the stations was calculated as described in Section 2.5.1 for the years 1992, 1993, and 2017. The available environmental (bottom water temperature, sediment CPE and TOC content, number of ice-free days) and community parameters (total Nematoda and Polychaeta abundance) between 1992, 1993, and 2017 were displayed with barplots. Subsequently, a CA was performed on relative family abundances (abundance of a family in a sample divided by the total abundance of all families in that sample) of Polychaeta from 1992, 1993, and 2017 in order to minimize errors due to the possible variation of species identification between the different sampling campaigns. The same was applied to Nematoda at the genus level, with data from Preben and Herman (2023).

Unidentified taxa were removed from both datasets, and validity of taxa names were checked on marinespecies.org.

A PERMANOVA was performed in order to test whether "time" (sampling years; categorical), "site" (previously delineated by SIMPROF on the 2017 data; categorical), and/or the "interaction between time and site" had a significant effect on the differences among Polychaeta and Nematoda community patterns between the different years ($p < 0.05$). All statistical analyses were performed using the computing environment R (Version 4.2.2; R Core Team, 2018) with the packages *vegan* (Oksanen et al., 2018) and *clustsig* (Whitaker, 2021).

3. Results
3.1. Environmental characteristics on the NEG shelf
Sea-ice-free days were lowest at the Glacier stations (0 ice-free days) and highest at the stations further away from shore (75–80 ice-free days; Figure S1). Water depth of the stations ranged between 140 m and 502 m. The shallowest stations were Station 122/129 (140 m), which were located on Belgica Bank, and Station 61/85/68 (156 m), located on a shoal directly in front of the glacier margin, peaking from a 300–500 m deep area. In 1992, the location of Station 61/85/68 was still covered by the 79°N Glacier (**Figure 1c**). In general, stations at the Glacier and in the Westwind Trough were shallower than the Norske Trough stations (206–315 m and 354–502 m, respectively). Bottom water salinity and temperature indicated the presence of water of Atlantic origin in the Norske Trough and at the Glacier (1.49–1.76°C; except for shallow Glacier Station 61/85/68), while stations in the Westwind Trough were influenced by cooler and fresher glacially modified water (0.69–0.87°C; Figure S2). The station on Belgica Bank was influenced by cold and fresher water.

Median grain size was lowest at all Glacier stations (9–10 µm) and highest on Belgica Bank (49 µm), followed by the Westwind Trough and outer Norske Trough (21 µm and 23 µm at Stations 19 and 36, and 20 µm and 48 µm at Stations 139 and 129, respectively; Figure S3a). Across the NEG shelf, the silt content was extremely high, with values of around 95% at the Glacier stations and about 80% at the other stations. Average concentrations of all measured pigment compounds in the upper 5 cm (CPE, as the sum of Chl *a* and phaeopigments, and fucoxanthin) were highest in the Westwind Trough, where the CPE range was 1.3–4.3 µg g^{-1} sediment (Figure S3b and c). At all other sites the range of values was 0.3–0.8 µg g^{-1} sediment, with similar ranges at the Glacier stations compared to the Norske Trough. TOC concentrations were very low at the Glacier stations (0.91–1.48 g m^{-2}) and highest in the Westwind Trough (2.96–3.81 g m^{-2}; Figure S3e). When single cell abundances (bacterial cells mL^{-1}; Figure S4) in all sediment sections, 0–5 cm, were summed, the abundances were lowest at all Glacier stations (2–4 × 10^9 cells cm^{-2}) and highest in the Westwind Trough (8 × 10^9–1 × 10^{10} cells cm^{-2}). Based on environmental variables, the SIMPROF analysis identified 4 spatially defined, distinct groups (Westwind Trough, 79°N Glacier, Norske Trough, and Belgica Bank; Figure S5).

3.2. Benthic processes
Total oxygen uptake was very low across all sites (**Figure 3**). Highest uptake rates were measured at Station 45 in the Dijmphna Sound, and at Station 139/139-L in the outer Norske Trough (2.17 and 1.64 mmol m^{-2} d^{-1}, respectively). Lowest uptake was measured at Stations 125 and 85 (around 1.2 mmol m^{-2} d^{-1}). Diffusive oxygen uptake was highest at Station 85/68-L (3.74 mmol m^{-2} d^{-1}) and lowest at Stations 93 and 125 (1.3 and 1 mmol m^{-2} d^{-1}, respectively).

Porewater nutrient concentrations were generally low (Figure S6). Sulfate and sulfide were not detected in the sampled cores. Overall, the Westwind Trough revealed
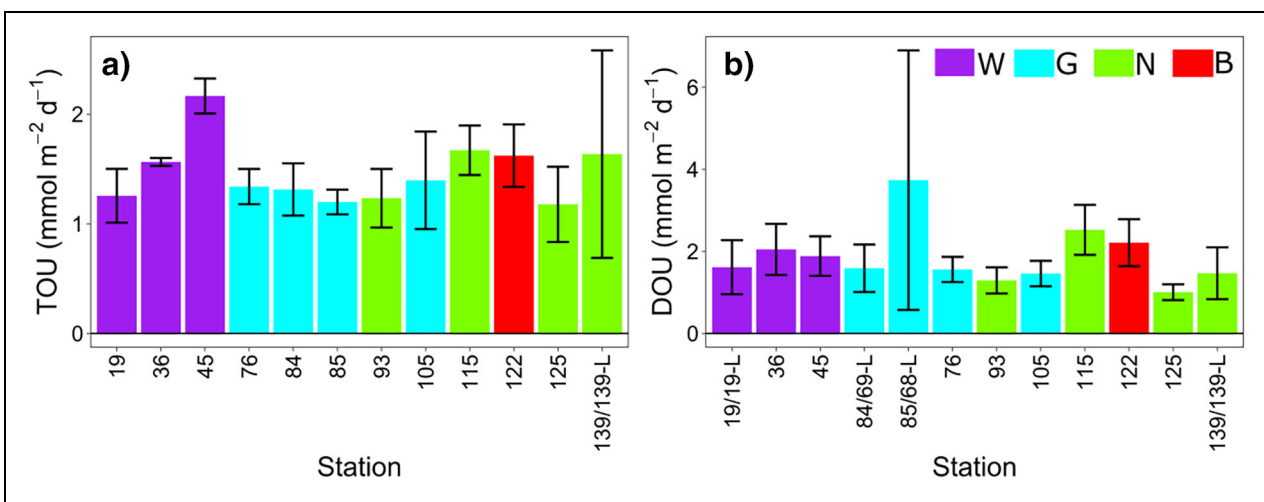

Figure 3. Ex situ total (TOU) and dissolved oxygen uptake (DOU) at the sediment-water interface. Means and standard deviations (error bars) for (a) TOU (n = 2–3, except for pooled station 139/139-L where n = 6) and (b) DOU (n = 10–12, except for pooled stations 19/19-L, 84/69-L, 85/68-L and 139/139-L, where n > 20) are given for each station. Colors represent the 4 sites statistically identified by the SIMPROF analysis based on standardized environmental data (Figure S5): Westwind Trough (W), 79°N Glacier (G), Norske Trough (N), and Belgica Bank (B).

different nutrient profiles than observed at all other sites. Ammonium concentrations were highest at Westwind Trough stations, where values increased with sediment depth (data not shown). At all other stations, ammonium concentrations were close to 0. Highest concentrations of nitrate were present at Norske Trough Stations 139 (103.0 mmol m^{-3}), 115 (89.9 mmol m^{-3}), and 125 (85.6 mmol m^{-3}). Nitrite was not detected at most of the Norske Trough stations, except Station 93. The range of nitrite concentrations at Westwind Trough stations was 0.3–0.6 mmol m^{-3}, while at the Glacier stations the range was 0–0.2 mmol m^{-3}. Phosphate was present overall in low concentrations of 3.2–14.4 mmol m^{-3}. DIC concentrations did not differ much across sites, varying between 5.58 mol m^{-3} and 8.89 mol m^{-3} across all sites. Silicate exhibited the highest concentrations in the Westwind Trough.

3.3. Benthic community characteristics

In total, 319 macrofaunal individuals from ex situ and 115 from in situ samples were identified, belonging to 109 and 62 distinct taxa, respectively. Polychaeta was the most represented phylum in abundance, with Maldanidae being the most abundant polychaete family. The most abundant macrofaunal species was *Boltenia ovifera* (Ascidiacea), with an average of 757 ind m^{-2} at Station 125, followed by juvenile Bivalvia at Station 19, with an average of 571 ind m^{-2}. All other macrofaunal taxa occurred with average densities lower than 571 ind m^{-2} (fewer than 4 individuals per sample). One of the triplicate samples at Glacier Station 85 did not contain any macrofaunal individuals except for a single colonial Bryozoan specimen (*Escharella sp.*), which could not be weighed due to its small size and fragility. Total macrofaunal densities were high (1,809–2,762 ind m^{-2}) at Station 122/129 on the Belgica Bank, at all stations in the Westwind Trough, at Station 125 in the Norske Trough, and at Glacier Station 76 (**Figure 4a**, Table S2). At all other stations macrofaunal densities were lower than 1,381 ind m^{-2}. Similar to density, biomass was the highest on Belgica Bank with 44.0 g m^{-2}, followed by the Westwind Trough (8.4–22.3 g m^{-2}) and lowest at the Glacier (0.8–5.7 g m^{-2}; **Figure 4e**). The non-parametric Kruskal–Wallis test performed on ex situ community parameters did not reveal significant differences among sites based on macrofaunal abundance (p = 0.08), Polychaeta abundance (p = 0.32), macrofaunal biomass (p = 0.05), and Polychaeta biomass (p = 0.09).

The highest densities of meiofauna were found in the Westwind Trough and on the Belgica Bank (2,707 ind cm^{-2} at Station 36 and 2,175 ind 10 cm^{-2} at Station 122; **Figure 4e**). The lowest densities were found at the Glacier stations (693–737 ind 10 cm^{-2}) and in the inner Norske Trough at Station 93 (466 ind 10 cm^{-2}). Across all stations, Nematoda comprised more than 85% of the meiofauna and their abundance pattern largely followed that of the total meiofaunal densities. Analyses on functional feeding groups did not show any pattern among stations (data not shown).

3.4. Relationship of benthic community parameters and environmental variables

Westwind and Norske Trough stations were distinct in the correspondence analysis plots for both macrofauna and meiofauna. In the CA based on macrofaunal density from ex situ MUC cores, the eigenvalues of the first and second correspondence axes (CA1 and CA2) accounted for 15% and 14% of the total variation each (Table S3, **Figure 5a**), together explaining 29% of the overall variation. The Westwind Trough stations correlated positively with higher CPE, TOC and single cell abundances, while the Norske Trough stations correlated negatively with these parameters. The Glacier stations grouped with the Norske Trough stations. The only vectors that were significantly correlated to the displayed ordination were CPE ($R^2 =$ 0.82, p = 0.007), salinity ($R^2 =$ 0.75, p = 0.010), and TOC ($R^2 =$ 0.67. p = 0.044).

The CA based on meiofaunal relative density showed that the Westwind Trough stations, similarly to macrofaunal communities, were characterized by higher CPE, TOC, and single cell abundances compared to the Norske Trough (Table S3, **Figure 5b**). Here, CA1 and CA2 together explained a much higher fraction of the overall station variance compared to macrofaunal relative density (CA1 = 34% and CA2 = 29%). Only CPE was significantly correlated with the displayed ordination ($R^2 =$ 0.74, p = 0.009).

3.5. Comparison to the early 1990s

Overall, Polychaeta densities were 4.8 times lower, and Nematoda densities 3.4 times higher, in 2017 compared to the early 1990s (**Figure 6a** and **b**). These differences were much more pronounced in the Westwind Trough (3,494 ind m^{-2} in the 1990s vs. 703 ind m^{-2} in 2017 for Polychaeta and 264 ind 10 cm^{-2} in the 1990s vs. 2,053 ind 10 cm^{-2} in 2017 for Nematoda) than in the Norske Trough (861 ind m^{-2} in the 1990s vs. 537 ind m^{-2} in 2017 for Polychaeta and 45 ind 10 cm^{-2} in the 1990s vs. 1,214 ind 10 cm^{-2} in 2017 for Nematoda). While TOC concentrations, as well as TOU, were relatively similar between the early 1990s and 2017 (0.31–1.45 g m^{-2} and 0.46–1.31 g m^{-2} for TOC in the early 1990s and in 2017, respectively; 11–148 µmol m^{-2} h^{-1} and 49–100 µmol m^{-2} h^{-1} for TOU in 1993 and in 2017, respectively; **Figure 6c** and **d**), CPE was 9.9 times higher in the early 1990s compared to 2017 (**Figure 6f**). Bottom water temperature across all stations sampled in 2017 was 2.8 times higher compared to the stations in the 1990s (**Figure 6e**).

A CA performed on abundances of Polychaeta families from the 1990s and 2017 displays that the stations from 2017 group on the left side of the ordination, while the stations from the 1990s group on the right side (**Figure 7a** and Table S4). In total, the first two axes explain 28.9% of the total variation. In particular, the stations on the Belgica Bank (122 and 129) clearly group further apart from all other stations.

The CA based on Nematoda genera shows a much stronger distinction between 2017 and 1993; the two years are clearly separated along the CA1, explaining
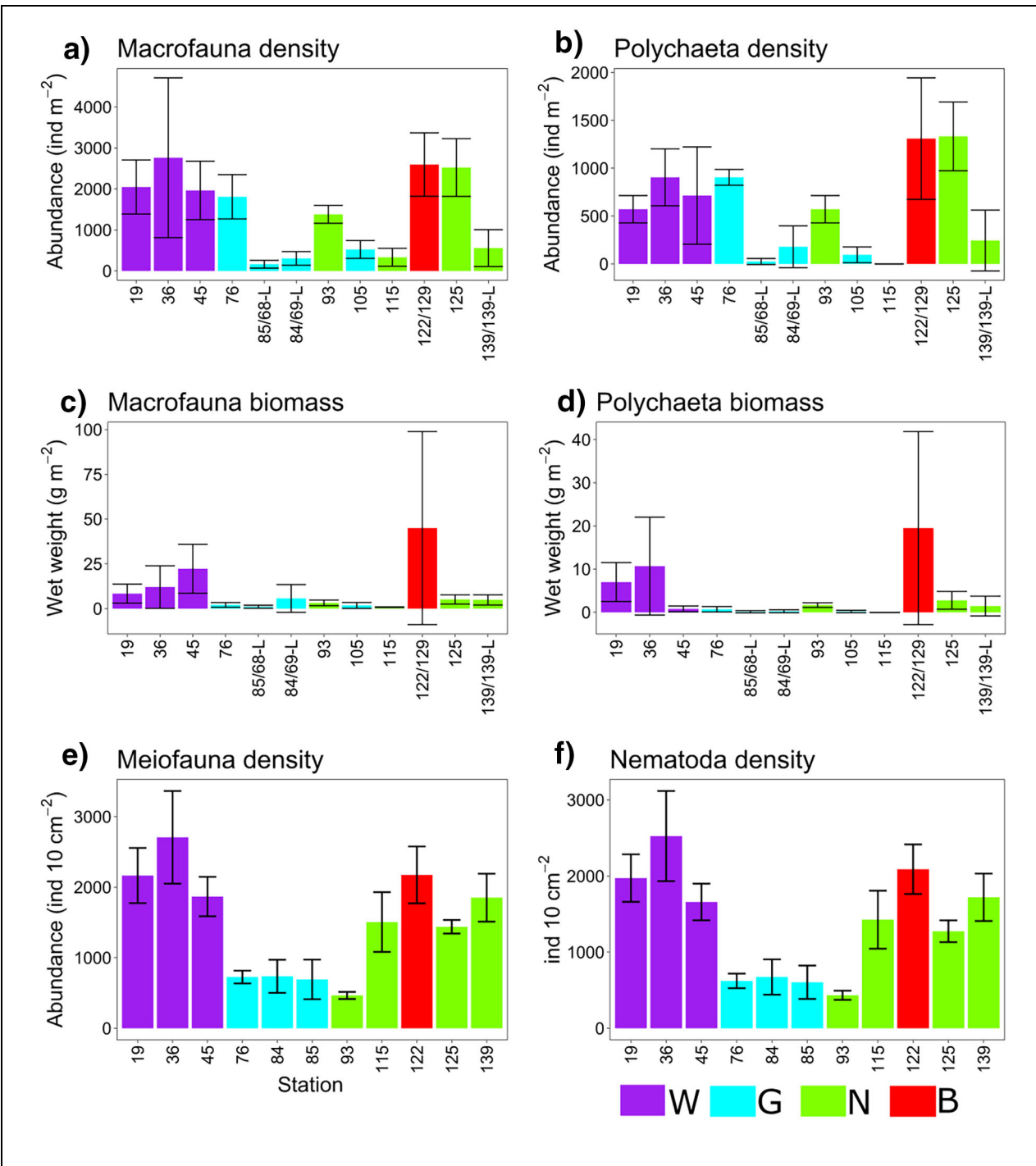
Figure 4. Macrofaunal and meiofaunal community parameters at each station. Means and standard deviations (error bars) are shown for (a, b, e, f) abundance (density) data and (c, d) biomass data (n = 3, except for pooled stations 85/68-L, 84/69-L, 122/129, 139/139-L, where n = 6). Colors represent the 4 sites statistically identified by the SIMPROF analysis based on standardized environmental data (Figure S5): Westwind Trough (W), 79°N Glacier (G), Norske Trough (N), and Belgica Bank (B). However, differences among sites based on these community parameters were not significant.

22.2% of the total variation (**Figure 7b** and Table S4). The number of observed genera was much higher in 2017, with 155 genera identified versus 79 genera identified in 1993. Along CA2, all stations except for the Westwind stations are grouped together, while there is a gradient for the Westwind stations from the Glacier toward the outer part of the

trough. In the 1990s, a distinction between the Westwind and the Norske Trough stations is visible along the CA2. A PERMANOVA performed on each of the datasets (Polychaeta and Nematoda) revealed significant differences based on time, site, and the interaction between time and site, with p-values < 0.03 (**Table 1**).
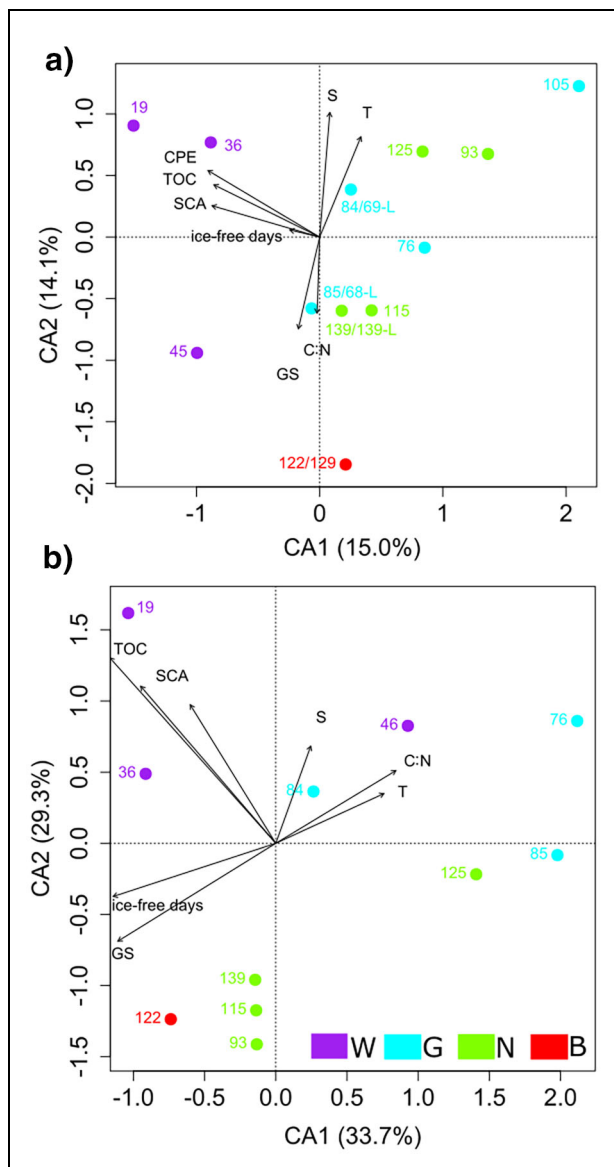
Figure 5. Visualization of the correspondence analysis for macrofaunal and meiofaunal communities with environmental parameters. Relative abundances of (a) macrofauna and (b) meiofauna with standardized environmental parameters fitted onto their ordination as supplementary variables. Colors represent the 4 sites statistically identified by the SIMPROF analysis based on standardized environmental data (Figure S5): Westwind Trough (W), 79°N Glacier (G), Norske Trough (N), and Belgica Bank (B). Tested environmental parameters are number of sea-ice-free days (ice-free days), sediment TOC:TN ratio (C:N), chloroplastic pigment equivalent (CPE), grain size (GS), single cell abundances (SCA), bottom water salinity (S) and temperature (T).

4. Discussion

4.1. Regional variations on the NEG shelf: Stronger pelagic-benthic coupling in the Westwind Trough

Marked regional differences in sediment organic matter content on the NEG shelf matched those in benthic biota. The Westwind Trough displayed the highest CPE and TOC content and highest single cell abundances. The strongest regional contrasts in abundance and biomass of benthic macrofauna and meiofauna were observed between the stations closest to the 79°N Glacier and the coast and those in the Westwind and outer Norske Trough area. Close to the Glacier, densities and biomass of macrofauna and meiofauna were the lowest. The similar responses of the different faunistic groups (macrofauna and meio-fauna) to the strongest contrasts in environmental variables (CPE and TOC content), and CPE being the only parameter that was significantly correlated to both ordinations, suggest that food availability is the main driver of the structure of these communities (**Figure 5**; Piepenburg et al., 1997). These results add to an extensive body of evidence linking spatial patterns in benthic community structure with those of pelagic productivity on Arctic shelves (Grebmeier and Barry, 1991; Ambrose and Renaud, 1995; Carroll et al., 2008).

Our data suggest that the reason for the lower abundance and biomass of benthic infauna in the areas closer to the 79°N Glacier is, as mentioned above, lower food input compared to the Westwind and outer Norske Troughs. These differences in food availability are similarly reflected in different benthic Foraminifera communities between the inner and the outer NEG shelf (Davies et al., 2023). Arctic benthic community structure is highly dependent on annual patterns of carbon export from primary production in the upper water column. In contrast, respiration of benthic communities on the NEG shelf is coupled to OM pulses (Rowe et al., 1997). This relationship is tightly driven by sea-ice dynamics. The stations in the Westwind Trough and outer Norske Trough are located in the marginal ice zone (Figure S1) where the number of sea-ice-free days was higher compared to the Glacier stations and the innermost Norske Trough Stations 93 and 105 which are close to the coast. Benthic communities feature especially high abundance and biomass at the marginal ice zone (Hoffmann et al., 2018), and higher faunal abundance, biomass, distinct community structure, and correspondence with higher values of CPE in these regions were also noted in the 1990s (Ambrose and Renaud, 1995; Piepenburg et al., 1997).

The elevated silicate concentrations in the pore water of Westwind Trough sediments are consistent with higher benthic fucoxanthin concentrations, indicating a higher diatom input in Westwind Trough. In addition, ammonium and nitrite concentrations in the porewater were higher in Westwind Trough compared to the other sites (Figure S6), indicative of higher mineralization rates. When oxygen is depleted, nitrate is used as the next suitable electron acceptor in microbial metabolism. Indeed, in Westwind Trough sediments, nitrate was depleted with depth (data not shown; see Braeckman and Felden, 2023), which could point to denitrification taking place in the deeper sediment layers. At all other sites, nitrate was not depleted with depth, and ammonium and silicate concentrations were much lower. These results indicate that nitrate is not consumed in the upper 20 cm of the sediment; that is, microbial metabolism is low. The results from benthic community structure and geochemistry
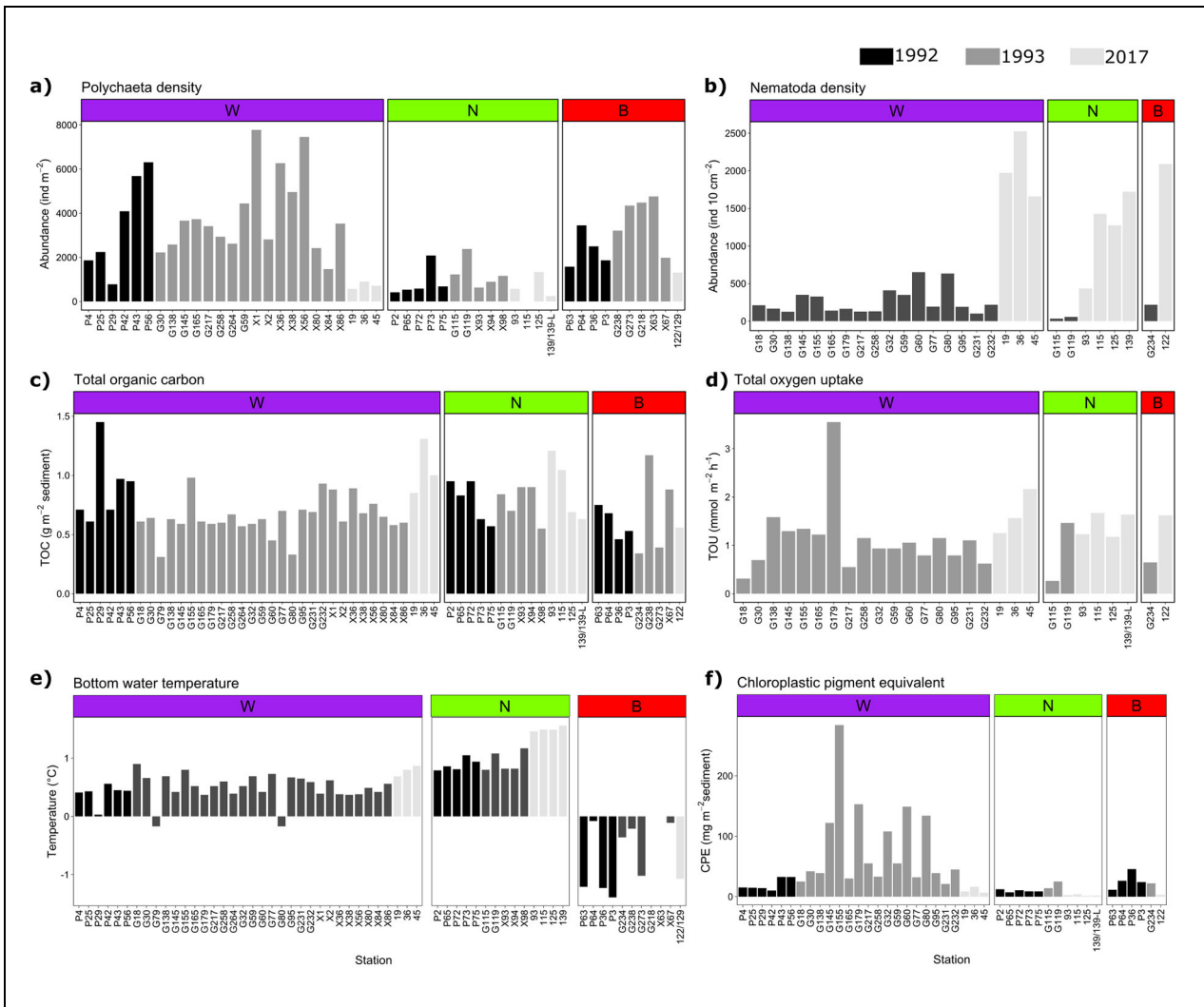
Figure 6. Comparison of benthic community parameters between 1992, 1993, and 2017. Plotted by station number are (a) Polychaeta density, (b) Nematoda density, (c) total organic carbon (TOC), (d) total oxygen uptake (TOU), (e) bottom water temperature, (f) chloroplastic pigment equivalent (CPE). Data from 1992 and 1993 were taken from Ambrose and Renaud (1995) and Piepenburg et al. (1997). Colors represent the sites statistically identified by the SIMPROF analysis based on standardized environmental data (Figure S5): Westwind Trough (W), Norske Trough (N), and Belgica Bank (B).

jointly suggest a tight pelagic-benthic coupling driven by higher diatom fluxes in the Westwind Trough area compared to the Glacier and inner Norske Trough areas. Indeed, primary production and export of algal cells during spring 1993 were also higher in the Westwind Trough, which is located within the NEW Polynya, compared to the Norske Trough, which was ice-covered during that time (Pesant et al., 1996; Pesant et al., 2000).

With benthic pigment concentrations being much higher in the Westwind Trough, the seafloor at this location could still be receiving a higher annual OM input. Uncalibrated ship-based fluorescence measurements in the upper water column during this study indicated similar phytoplankton biomass in the water column of both troughs during the sampling period (Kanzow and Rohardt, 2017), but this similarity likely reflected a consequence of the timing of sampling relative to bloom and/or vertical flux phenologies in the two regions. Another mechanism

could be a "decoupling" of the benthic environment from the pelagic in the Norske Trough due to higher zooplankton grazing (Ambrose and Renaud, 1995). Ashjian et al. (1995) observed that pelagic grazing rates greatly exceeded primary production in both the Westwind and Norske troughs, but especially in the Norske Trough, consistent with reduced food input for the benthos (Ambrose and Renaud, 1995). Possibly pelagic mineralization took place before OM could settle, leaving a lower fraction of the surface production to reach the seafloor in this area. In contrast to the stations within the Norske Trough, the station located on the Belgica Bank showed benthic abundances and biomasses similar to the Westwind Trough, as well as higher benthic remineralization rates (**Figures 3**, **4**, and S5), which are most likely due to the shallow depth receiving more settled OM than a deeper trough. Similarly, the stations in the Westwind Trough were shallower (206–315 m) than those in the Norske Trough (354–502 m),
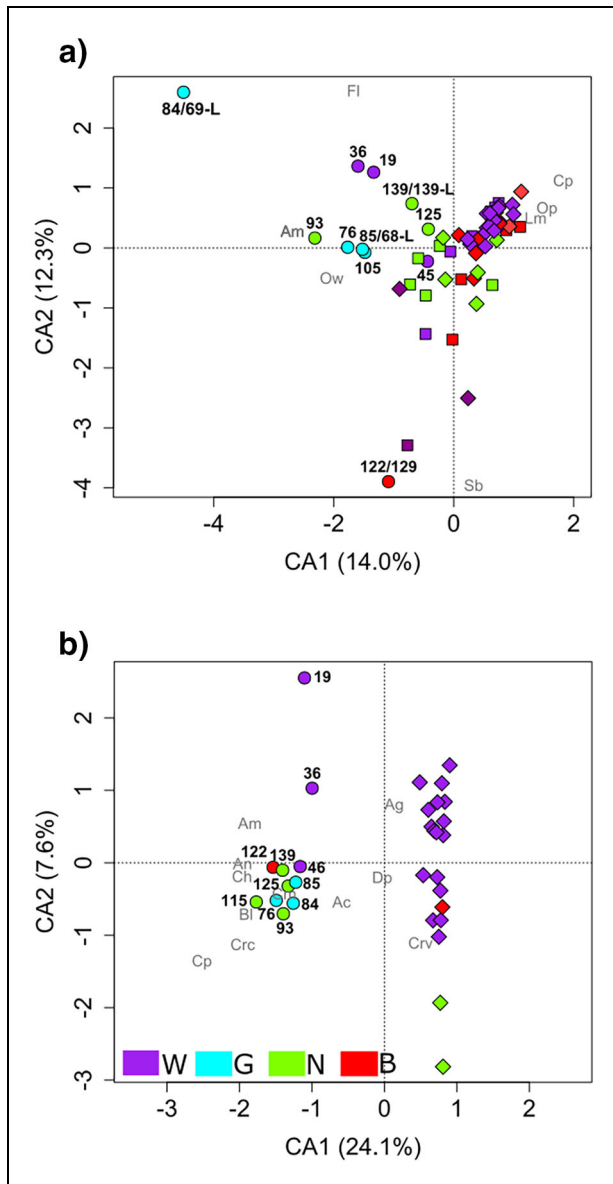
Figure 7. Visualization of the correspondence analysis for Polychaeta and Nematoda with sampling year. Relative abundances of (a) Polychaeta (family level) and (b) Nematoda (genus level) from 1992 (squares), 1993 (diamonds), and 2017 (circles). Symbol colors represent the 4 sites statistically identified by the SIMPROF analysis based on standardized environmental data (Figure S5): Westwind Trough (W), 79°N Glacier (G), Norske Trough (N), and Belgica Bank (B). Abbreviations for the most abundant taxa (Polychaeta families >500 ind m^{-2} and Nematoda genera >30 ind 10 cm^{-2}) are depicted in gray font; station numbers from 2017, in black font. Polychaeta families in (a) are Ampharetidae (Am), Capitellidae (Cp), Flabelligeridae (Fl), Lumbrineridae (Lm), Opheliidae (Op), Oweniidae (Ow) and Sabellidae (Sb). Nematoda genera in (b) are *Acantholaimus* (Ac), *Aegialoalaimus* (Ag), *Amphimonhystrella* (Am), *Anoplostoma* (An), *Bolbolaimus* (Bl), Chromadorita (Ch), *Campylaimus* (Cm), *Capsula* (Cps), *Ceramonema* (Cr), *Cricohalalaimus* (CrC), *Cervonema* (Crv), and *Diplopeltula* (Dp).

possibly explaining more OM settling at this site, with a shorter distance to the seafloor, and hence fueling a richer benthic community.

Both benthic diffusive and total oxygen uptake rates were very low, showing little differentiation among the sites. In general, benthic stations under more productive surface waters on Arctic shelves exhibit higher benthic process rates than stations in less productive regions (Grebmeier and Barry, 1991; Graf et al., 1995; Renaud et al., 2008; Grebmeier et al., 2015). Seasonal patterns in vertical flux of phytodetritus can also be tightly linked with temporal patterns in benthic oxygen utilization (Renaud et al., 2007). Thus, the overall low rates observed here may be representing minimum rates, while a rate measured after a bloom would result in higher rates. By late September–October when these measurements were performed, the spatial variation in seasonal carbon deposition in the area was no longer apparent in processes expected to respond more rapidly than other benthic parameters such as community structure or sediment geochemistry (McMahon et al., 2006; Renaud et al., 2008; Morata et al., 2015). Moreover, sediment oxygen uptake is usually dominated by microbial communities that react more dynamically to seasonal food input than macrofauna and meiofauna (Piepenburg et al., 1995); therefore, a seasonal signal in TOU might have faded toward autumn, while differences in macrofaunal and meiofaunal community structures usually persist over longer time scales.

4.2. Comparing NEG to other Arctic shelves: An oligotrophic outflow shelf

The NEG shelf is an Arctic outflow shelf, transporting Arctic Water into the North Atlantic. Primary production on Arctic outflow shelves is typically highly seasonal, quickly nutrient-limited, and highly variable spatially and interannually (Carmack and Wassmann, 2006). Pelagic primary production rates on the NEG shelf are 1–2 orders of magnitude lower than those on productive inflow shelves such as the shallow Chukchi Sea and deep Barents Sea (Pabi et al., 2008). This lower primary production is also reflected in the amount of fresh OM that arrives at the seafloor. The maximum sediment CPE content observed in this study was indeed an order of magnitude lower than the maximum CPE content in sediments of the shallow Chukchi Sea (McTigue et al., 2015) and Barents Sea at comparable depths to this study (Morata and Renaud, 2008). The overall low Chl *a*:phaeopigment ratios on the NEG shelf (Figure S3d) suggest that OM was in a degraded state. Presumed low input of fresh OM is also reflected in low benthic activity, with TOU values across the NEG shelf comparable to those observed in the 1990s (0.31–3.55 mmol m^{-2} d^{-1} in Piepenburg et al., 1997; 0.72–6.72 mmol m^{-2} d^{-1} in Rowe et al., 1997) and in the deep Arctic Fram Strait (0.5–5.1 mmol m^{-2} d^{-1}; Hoffmann et al., 2018). In contrast, at similar depths (200–500 m) in the inflow Chukchi Sea and Svalbard region, TOU is generally up to 10 times higher (Bourgeois et al., 2017). These comparisons confirm the previous report about this outflow region being oligotrophic (Rowe et al., 1997).

Table 1. Results of the PERMANOVA performed on the community parameters of Polychaeta and Nematoda densities from 1992, 1993, and 2017

Factor Tested	Df[a]	Sum of Squares	R^2	F	Pr(>F)
Polychaeta					
Time	2	2.49	0.17	7.15	0.00
Site	5	2.92	0.20	3.37	0.00
Time and site	5	1.28	0.09	1.48	0.04
Residual	45	7.82	0.54	NA[b]	NA
Total	57	14.51	1.00	NA	NA
Nematoda					
Time	1	2.85	0.40	23.78	0.00
Site	3	0.80	0.11	2.21	0.01
Time and site	2	0.53	0.08	2.21	0.02
Residual	24	2.88	0.41	NA	NA
Total	30	7.06	1.00	NA	NA

[a]Degrees of freedom.

[b]Not applicable.

In accordance, the abundance of macrofauna on the NEG shelf was generally low compared to Arctic inflow shelf regions. Locations where densities were the highest (all stations in the Westwind Trough, and stations in the outer Norske Trough, far from the 79°N Glacier) featured similar densities to sites with low food availability recorded in Svalbard fjords (76–250 m water depths; Włodarska-Kowalczuk and Pearson, 2004) and the western Barents Sea (Carroll et al., 2008). Although the spatial scale in our study and distances between stations were large (55–150 km distances between stations on the shelf), compositional differences among benthic communities were relatively small (**Figure 5**). The circulation of AIW in the trough system might lead to very similar hydrographic conditions among stations. In contrast, benthic communities along a transect of only a few kilometers in the glacial fjord of Kongsfjorden featured conspicuous differences (Włodarska-Kowalczuk et al., 2005; Bourgeois et al., 2016). Open-shelf benthic systems, however, have higher species diversity and higher numbers of rare species compared to fjord systems (Włodarska-Kowalczuk et al., 2012), and differences among sites emerge at much larger distances (Cochrane et al., 2012), which is in accordance with our findings.

Surprisingly, this study did not show clear dominance patterns in the macrofaunal communities, but all species were present in low abundance (<4 ind. 0.007 m^{-2}). The same pattern was observed in the samples from the early 1990s (Ambrose and Renaud, 1995). Often, benthic communities are dominated by a few species in high densities (e.g., Włodarska-Kowalczuk and Pearson, 2004; Blanchard et al., 2013); however, the infaunal communities on the NEG shelf appear to be highly diverse with very low densities. This finding agrees with the observation that North Greenland features comparatively high species richness

among the Arctic marine ecoregions (Piepenburg et al., 2011). Meiofaunal communities in this study, on the other hand, were strongly dominated by nematodes, as is usually the case in other benthic ecosystems (Gerlach, 1971; Włodarska-Kowalczuk et al., 2016; Hoffmann et al., 2018; Veit-Köhler et al., 2018).

4.3. A possible weakening of pelagic–benthic coupling on the NEG shelf since the 1990s
We found strong contrasts in physical parameters of the sediment as well as in community structure between the early 1990s and 2017 (present study). A 0.5°C temperature increase of the bottom water in the Norske Trough in 2000–2016 compared to 1979–1999 (Schaffer et al., 2017; see also **Figure 6e**) and lower sediment pigment content (**Figure 6f**) were striking. A strong influence of warm Atlantic Water and absence of sea ice can be related to a higher amount of degraded material reaching the seafloor, due to a more active microbial loop and higher grazing pressure in the pelagic environment (Dybwad et al., 2022). CPE concentrations for the upper 2 cm of the sediment varied between 7.2 mg m^{-2} and 45.6 mg m^{-2} across the whole NEG shelf between July and August in the early 1990s (Ambrose and Renaud, 1995), while in this study (conducted in September–October, 2017), highest concentrations were found in the Westwind Trough, with values of 7.38–18.0 mg m^{-2}. At all other sites, CPE concentrations were close to 0. While this pattern could reflect a seasonal effect, the consistently low macrofaunal densities in 2017 suggest that a seasonal effect is not the only reason, because macrofaunal community structure reflects ecosystem processes on a longer time scale, especially in oligotrophic areas like the NEG shelf.

Macrofaunal abundances in 1992 were nearly 5× higher than we observed in 1992. In contrast, Nematoda

abundances were 3.4 times higher in 2017 than recorded in 1993, and a much higher diversity of nematode genera was observed in 2017 (157 identified in 2017 vs. 77 identified in 1993). Nematoda in deep-sea polar regions have been shown to prefer bacteria over fresh phytoplankton (Ingels et al., 2010), so the shift observed here could be linked with lower quality as well as quantity of the food supply from surface waters. The CAs based on meiofaunal and macrofaunal abundances (**Figure 5**) showed less variation in benthic community structure across the shelf in 2017 compared to the strong spatial differences between the Westwind and Norske troughs in the 1990s (Piepenburg et al., 1997), suggesting a homogenization of the shelf communities. This change in an already oligotrophic shelf system appears to indicate a system more closely resembling a deep-sea community, with few hotspots of food supply to the seafloor and predominance of smaller biota in sediments (e.g., Górska et al., 2020). Similarly, during the campaigns in the 1990s benthic foraminifera communities across the NEG shelf were dominated by calcified species, while in 2017 agglutinated species were dominating (Davies et al., 2023). The spread of stations in the CA plot, however, also suggests that between-study differences in taxonomic identification of fauna, particularly for nematodes, may have contributed to variability. Stations are completely separated by sampling period and show a similar latitudinal gradient, which suggests either wholesale community changes such that even the most oligotrophic stations in both sampling occasions shifted or an inconsistency in naming of organisms. This "identifier bias" is not uncommon in the literature (e.g., Bluhm et al., 2011). We took several measures to reduce potential bias, such as checking and harmonizing species names on marinespecies.org for both datasets, selecting coarse taxonomic resolutions (family level for polychaetes and genus level for nematodes), and using relative abundance for the data analysis (taxon number divided by total number of individuals at the respective station).

Some of the differences between the early 1990s and our study may be a consequence of sampling season or simply intra-annual variability, especially with regard to sea-ice cover. Samples were taken during different months in both studies (March–August in 1992/1993 vs. September–October in 2017). Upon reaching the seafloor, phytodetritus can be consumed rapidly by the benthos (Morata et al., 2015) and a pigment signal from a spring bloom in surface sediments can fade with time. Spring bloom timing may also have changed due to differences in seasonality in ice cover. An earlier bloom in 2017 may have resulted in an earlier benthic food consumption, which would in turn lead to a lower detection of pigment concentrations late in the year than it did before. Sejr et al. (2000), for example, showed an increase in macrofaunal abundance in Young Sound from mid-July to mid-August, coupled with changes in primary production. The low Chl *a*:phaeopigment ratios in the sediment from our study indicate that sediment pigments reflect older or more processed phytodetritus. Assuming a lack of secondary bloom, the pigment content of the sediment would be expected to be higher in July–August and more depleted in September–October.

Our observations of slightly higher oxygen uptake in 2017 compared to 1993 (63.7 μmol m^{-2} h^{-1} vs. 44.8 μmol m^{-2} h^{-1}) appears to contradict the assumption that an earlier spring bloom during the 1993 sampling campaign would fuel a rapid consumption and oxygen uptake in contrast to 2017. Although polychaete recruitment was seasonally variable, no synchrony between recruitment and pulsed sedimentation of organic material was detected (Ambrose and Renaud, 1997). Even if seasonal signals can be detected in oxygen uptake rates (Morata et al., 2015), seasonal patterns are not usually integrated in the community structure of macrofauna and meiofauna in the Arctic (Kędra et al., 2012; Berge et al., 2015; Włodarska-Kowalczuk et al., 2016).

What, then, may be responsible for the observed changes across this shelf region over the span of 25 years? As observed everywhere in the Arctic, the extent of sea-ice cover on the NEG shelf is shrinking, with an increasing ice-free period during summer (Stroeve et al., 2012). On the NEG shelf, however, interannual variability of sea-ice concentration evaluated between 1995 and 2017 was large, showing no obvious trend. However, the thickness of sea ice transported onto the NEG shelf through Fram Strait has decreased drastically since the last decade (Spreen et al., 2020; Sumata et al., 2022). There is an increasing influence of freshwater layering on the NEG shelf (Sejr et al., 2017), which may lead to decreased nutrient concentrations (Li et al., 2009) and subsequent lower primary production, ultimately resulting in lower export of OM to the seafloor (von Appen et al., 2021). Moreover, the NØIB in the south of the 79°N Glacier, a land-fast ice barrier that keeps the NEW Polynya in place and prevents calving of the glacier, is breaking up seasonally more often due to increasing summer temperatures in the area (Reeh et al., 2001; Smith and Barber, 2007). The ice barrier prevented surface currents from advecting sea ice into the Westwind Trough, which kept an open water area in place. In the early 1990s, this polynya was strongly related to abundance patterns of benthos and was characterized by tight pelagic-benthic coupling in the Westwind Trough, compared to a weaker pelagic-benthic coupling in the Norske Trough (Ambrose and Renaud, 1995; Brandt, 1995; Hobson et al., 1995; Piepenburg et al., 1997). Without the NØIB barrier, the sea-ice cover across the NEG shelf becomes more variable, likely reducing the differentiation between the Westwind Trough and Norske Trough. Pelagic-benthic coupling may have weakened in the region due to a more recurrent break-up of the polynya (ISSI, 2008; Reeh, 2017).

One scenario of the effects of shrinking ice cover in the Arctic is that the longer exposure to sunlight will result in a longer season for phytoplankton growth and higher production rates (Arrigo et al., 2008), thus to a higher food input for the benthos. This study indicates that a different scenario might be happening on the NEG shelf. Due to climate warming, Arctic sea ice melts earlier in the year, and the ice-free period is prolonged (Overland and Wang, 2013). Primary production starts earlier in the year and

sunlight could be available to phytoplankton for a longer period of time, but primary production might not be high throughout this period as nutrients would be consumed earlier during peak bloom in early spring (Wassmann and Reigstad, 2011). Lower nutrient concentrations favor smaller phytoplankton with lower carbon export efficiency (Li et al., 2009). During the early 1990s massive assemblages of under-ice algae were recorded underneath first-year ice sheets on the NEG shelf, dominated by the diatom *Melosira arctica* (Gutt, 1995), which could have provided important food pulses for benthic communities during ice melt in spring during that time (Bauerfeind et al., 1997).

The wider time window for pelagic primary production and increasing stratification increases in turn the time available for heterotrophic pelagic consumers to exploit this primary resource by extended grazing periods and population growth (Olli et al., 2007). Accordingly, the current Arctic marine ecosystem, characterized locally by highly seasonal and short-term "pulses" of organic carbon production and deposition (Grebmeier and Barry, 1991), may shift to one where a smaller share of primary production may be available for export. If the input of warmer AIW introduces more Atlantic zooplankton species onto the NEG shelf, enhanced grazing could lead to a "decoupling" of the benthic system from the pelagic productivity. In fact, the carbon demand of pelagic heterotrophs on the NEG shelf was reported to exceed the estimated local primary production (Carmack and Wassmann, 2006). Such an imbalance could also have led to the homogenization of the benthic communities between the Norske and the Westwind Trough, compared to the early 1990s when differences between benthic community compositions were far more conspicuous. A shift away from pelagic-benthic coupling has been predicted for Arctic ecosystems (Grebmeier and Barry, 1991) and has been reported for the Northern Bering Sea, with a northward shift of the pelagic-dominated ecosystem that was previously limited to the southeastern Bering Sea (Grebmeier et al., 2006). Our results are consistent with the new scenario of reduced food input to the benthos, although the mechanism proposed here is speculative. The extent to which our findings of change in the region are due to broader ecosystem change to be found throughout the Arctic is unclear. Just as in the early 1990s, this study provides only a snapshot of pigment concentrations and benthic community parameters. Annual patterns need to be further resolved empirically in order to be able to state clear conclusions about climate change-related ecosystem shifts.

5. Conclusions

Revisiting the NEG shelf 25 years after the first benthic studies there has demonstrated that, despite the decrease in sea-ice cover and variability in the NEW Polynya, the area is still an oligotrophic Arctic outflow shelf. Macrobenthic and meiobenthic communities in 2017 exhibited high diversity across the shelf but low abundances and activity. Pelagic-benthic coupling remained most pronounced in Westwind Trough, while food availability was lowest close to the 79°N Glacier. However, sediment pigment content had decreased markedly since the early 1990s, along with a reduction in polychaete densities, while nematode density and diversity had increased. These results may be due to a weakening of pelagic-benthic coupling, leading to input of pelagic organic matter in a lower quantity and more degraded state, possibly driven by a local change in the strength of the NEW Polynya or the stratification regime.

Data accessibility statement

All data used were published on PANGAEA (www.pangaea.de) and cited within this manuscript.

Supplemental files

The supplemental files for this article can be found as follows:

Tables S1–S4. Figures S1–S6. docx

Competing interests

The authors declare no competing interests.

Author contributions

UB, FW, JF planned and conducted the fieldwork and in situ measurements. YVB analyzed single cell abundances, counted and identified macrofaunal abundances and determined their biomass. UB and MWK contributed to macrofaunal identifications. LL and LDCM counted and identified meiofauna and Nematoda. TK provided sea-ice data and their interpretation. PER and WGA provided data from the early 1990s and their interpretation. YVB

analysed all data. YVB, PER, and UB drafted this manuscript. All authors revised and contributed to its finalization and approved of the submitted version.

References

Ambrose, WG, **Renaud, PE**. 1995. Benthic response to water column productivity patterns: Evidence for benthic-pelagic coupling in the Northeast Water Polynya. *Journal of Geophysical Research: Oceans* **100**(C3): 4411–4421. DOI: http://dx.doi.org/10.1029/94JC01982.

Ambrose, WG, **Renaud, PE**. 1997. Does a pulsed food supply to the benthos affect polychaete recruitment patterns in the Northeast Water Polynya? *Journal of Marine Systems* **10**(1–4): 483–495. DOI: http://dx.doi.org/10.1016/S0924-7963(96)00053-X.

April, A, **Montpetit, B**, **Langlois, D**. 2019. Linking the open water area of the North Open Water Polynya to climatic parameters using a multiple linear regression prediction model. *Atmosphere-Ocean* **57**(2): 91–100. DOI: http://dx.doi.org/10.1080/07055900.2019.1598332.

Ardyna, M, **Babin, M**, **Gosselin, M**, **Devred, E**, **Rainville, L**, **Tremblay, J-É**. 2014. Recent Arctic Ocean Sea ice loss triggers novel fall phytoplankton blooms. *Geophysical Research Letters* **41**(17): 6207–6212. DOI: http://dx.doi.org/10.1002/2014GL061047.

Arndt, JE, **Jokat, W**, **Dorschel, B**, **Myklebust, R**, **Dowdeswell, JA**, **Evans, J**. 2015. A new bathymetry of the Northeast Greenland continental shelf: Constraints on glacial and other processes. *Geochemistry, Geophysics, Geosystems* **16**(10): 3733–3753. DOI: http://dx.doi.org/10.1002/2015GC005931.

Arrigo, KR, **van Dijken, G**, **Pabi, S**. 2008. Impact of a shrinking Arctic ice cover on marine primary production. *Geophysical Research Letters* **35**(19). DOI: http://dx.doi.org/10.1029/2008GL035028.

Arrigo, KR, **van Dijken, GL**. 2015. Continued increases in Arctic Ocean primary production. *Progress in Oceanography* **136**: 60–70. DOI: http://dx.doi.org/10.1016/j.pocean.2015.05.002.

Ashjian, CJ, **Smith, SL**, **Lane, PVZ**. 1995. The Northeast Water Polynya during summer 1992: Distribution and aspects of secondary production of copepods. *Journal of Geophysical Research: Oceans* **100**(C3): 4371–4388. DOI: http://dx.doi.org/10.1029/94JC02199.

Barnhart, KR, **Miller, CR**, **Overeem, I**, **Kay, JE**. 2016. Mapping the future expansion of Arctic open water. *Nature Climate Change* **6**: 280–285. DOI: http://dx.doi.org/10.1038/nclimate2848.

Bauerfeind, E, **Garrity, C**, **Krumbholz, M**, **Ramseier, RO**, **Voß, M.** 1997. Seasonal variability of sediment trap collections in the Northeast Water Polynya. Part 2. Biochemical and microscopic composition of sedimenting matter. *Journal of Marine Systems* **10**: 371–389. DOI: https://doi.org/10.1016/S0924-7963(96)00069-3.

Berge, J, **Daase, M**, **Renaud, PE**, **Ambrose, WG**, **Darnis, G**, **Last, KS**, **Leu, E**, **Cohen, JH**, **Johnsen, G**, **Moline, MA**, **Cottier, F**, **Varpe, Ø**, **Shunatova, N**, **Bałazy, P**, **Morata, N**, **Massabuau, J-C**, **Falk-Petersen, S**, **Kosobokova, K**, **Hoppe, CJM**, **Węsławski, JM**, **Kukliński, P**, **Legeżyńska, J**, **Nikishina, D**, **Cusa, M**, **Kędra, M**, **Włodarska-Kowalczuk, M**, **Vogedes, D**, **Camus, L**, **Tran, D**, **Michaud, E**, **Gabrielsen, TM**, **Granovitch, A**, **Gonchar, A**, **Krapp, R**, **Callesen, TA**. 2015. Unexpected levels of biological activity during the polar night offer new perspectives on a warming Arctic. *Current Biology* **25**(19): 2555–2561. DOI: http://dx.doi.org/10.1016/j.cub.2015.08.024.

Beszczynska-Möller, A, **Fahrbach, E**, **Schauer, U**, **Hansen, E**. 2012. Variability in Atlantic water temperature and transport at the entrance to the Arctic Ocean, 1997–2010. *ICES Journal of Marine Science* **69**(5): 852–863. DOI: http://dx.doi.org/10.1093/icesjms/fss056.

Blanchard, AL, **Parris, CL**, **Knowlton, AL**, **Wade, NR.** 2013. Benthic ecology of the northeastern Chukchi Sea. Part I. Environmental characteristics and macrofaunal community structure, 2008–2010. *Continental Shelf Research* **67**: 52–66. DOI: http://dx.doi.org/10.1016/j.csr.2013.04.021.

Bluhm, BA, **Ambrose, WG**, **Bergmann, M**, **Clough, LM**, **Gebruk, AV**, **Hasemann, C**, **Iken, K**, **Klages, M**, **MacDonald, IR**, **Renaud, PE**, **Schewe, I**, **Soltwedel, T**, **Włodarska-Kowalczuk, M.** 2011. Diversity of the Arctic deep-sea benthos. *Marine Biodiversity* **41**: 87–107. DOI: http://dx.doi.org/10.1007/s12526-010-0078-4.

Bodur, YV, **Deja, K**, **Górska, B**, **Kędra, M**, **Kukliński, P**, **Legeżyńska, J**, **Pawlowska, J**, **Ronowicz, M**, **Włodarska-Kowalczuk, M**, **Braeckman, U.** 2023a. Benthic macrofauna and foraminifera (>500 μm) diversity, abundance and biomass on the Northeast Greenland (NEG) shelf sediments during POLARSTERN cruise PS109. PANGAEA. DOI: https://doi.pangaea.de/10.1594/PANGAEA.959134.

Bodur, YV, **Felden, J**, **Braeckman, U.** 2023b. Single prokaryotic cell abundances of the Northeast Greenland (NEG) shelf sediments from POLARSTERN cruise PS109. PANGAEA. DOI: https://doi.pangaea.de/10.1594/PANGAEA.959552.

Bourgeois, S, **Archambault, P**, **Witte, U.** 2017. Organic matter remineralization in marine sediments: A Pan-Arctic synthesis. *Global Biogeochemical Cycles* **31**(1): 190–213. DOI: http://dx.doi.org/10.1002/2016GB005378.

Bourgeois, S, **Kerhervé, P**, **Calleja, MLl**, **Many, G**, **Morata, N.** 2016. Glacier inputs influence organic matter composition and prokaryotic distribution in a high Arctic fjord (Kongsfjorden, Svalbard). *Journal of Marine Systems* **164**: 112–127. DOI: http://dx.doi.org/10.1016/j.jmarsys.2016.08.009.

Bourke, RH, **Newton, JL**, **Paquette, RG**, **Tunnicliffe, MD.** 1987. Circulation and water masses of the East Greenland shelf. *Journal of Geophysical Research: Oceans* **92**(C7): 6729–6740. DOI: http://dx.doi.org/10.1029/JC092iC07p06729.

Braeckman, U. 2023a. Grain size analysis of the Northeast Greenland (NEG) shelf sediments from POLARSTERN cruise PS109. PANGAEA. DOI: https://doi.pangaea.de/10.1594/PANGAEA.959546.

Braeckman, U. 2023b. Porosity of the Northeast Greenland (NEG) shelf sediments from POLARSTERN cruise PS109. PANGAEA. DOI: https://doi.pangaea.de/10.1594/PANGAEA.959550.

Braeckman, U. 2023c. Sedimentary pigments on the Northeast Greenland (NEG) Shelf from Polarstern cruise PS109. PANGAEA. DOI: https://doi.pangaea.de/10.1594/PANGAEA.959548.

Braeckman, U. 2023d. Total organic nitrogen (TON) and total organic carbon (TOC) concentration of the Northeast Greenland (NEG) shelf sediments from POLARSTERN cruise PS109. PANGAEA. DOI: https://doi.pangaea.de/10.1594/PANGAEA.959554.

Braeckman, U, Felden, J. 2023. Porewater nutrients of the Northeast Greenland (NEG) shelf sediments from POLARSTERN cruise PS109. PANGAEA. DOI: https://doi.pangaea.de/10.1594/PANGAEA.959549.

Braeckman, U, Janssen, F, Lavik, G, Elvert, M, Marchant, H, Buckner, C, Bienhold, C, Wenzhöfer, F. 2018. Carbon and nitrogen turnover in the Arctic deep sea: In situ benthic community response to diatom and coccolithophorid phytodetritus. *Biogeosciences Discussions* **15**: 6537–6557. DOI: http://dx.doi.org/10.5194/bg-2018-264.

Braeckman, U, Wenzhöfer, F. 2023. Ex situ total oxygen uptake of the Northeast Greenland (NEG) shelf sediments from POLARSTERN cruise PS109. PANGAEA. DOI: https://doi.pangaea.de/10.1594/PANGAEA.959553.

Brandt, A. 1995. Peracarid fauna (Crustacea, Malacostraca) of the Northeast Water Polynya off Greenland: Documenting close benthic-pelagic coupling in the Westwind Trough. *Marine Ecology Progress Series* **121**: 39–51. DOI: http://dx.doi.org/10.3354/meps121039.

Carmack, E, Wassmann, P. 2006. Food webs and physical–biological coupling on pan-Arctic shelves: Unifying concepts and comprehensive perspectives. *Progress in Oceanography* **71**(2–4): 446–477. DOI: http://dx.doi.org/10.1016/j.pocean.2006.10.004.

Carroll, ML, Denisenko, SG, Renaud, PE, Ambrose Jr, WG. 2008. Benthic infauna of the seasonally ice-covered western Barents Sea: Patterns and relationships to environmental forcing. *Deep Sea Research Part II: Topical Studies in Oceanography* **55**: 2340–2351.

Cochrane, SKJ, Pearson, TH, Greenacre, M, Costelloe, J, Ellingsen, IH, Dahle, S, Gulliksen, B. 2012. Benthic fauna and functional traits along a Polar Front transect in the Barents Sea—Advancing tools for ecosystem-scale assessments. *Journal of Marine Systems* **94**: 204–217. DOI: http://dx.doi.org/10.1016/j.jmarsys.2011.12.001.

Comiso, JC, Meier, WN, Gersten, R. 2017. Variability and trends in the Arctic Sea ice cover: Results from

different techniques. *Journal of Geophysical Research: Oceans* **122**(8): 6883–6900. DOI: http://dx.doi.org/10.1002/2017JC012768.

Da Costa Monteiro, L, Lins, L, Braeckman, U. 2023a. Benthic meiofauna diversity on the Northeast Greenland (NEG) shelf during POLARSTERN cruise PS109. PANGAEA. DOI: https://doi.pangaea.de/10.1594/PANGAEA.959357.

Da Costa Monteiro, L, Lins, L, Braeckman, U. 2023b. Nematoda diversity and functional feeding groups on the Northeast Greenland (NEG) shelf during POLARSTERN cruise PS109. PANGAEA. DOI: https://doi.pangaea.de/10.1594/PANGAEA.959351.

Dalsgaard, T, Nielsen, LP, Brotas, V, Viaroli, P, Underwood, G, Nedwell, D, Sundbäck, K, Rysgaard, S, Miles, A, Bartoli, M, Dong, L, Thornton, D, Ottosen, L, Castaldelli, G, Risgaard-Petersen, N. 2000. *Protocol handbook for NICE-Nitrogen cycling in estuaries: A project under the EU research programme.* Silkeborg, Denmark: Marine Science and Technology Program (MAST III), National Environmental Research Institute.

Davies, J, Lloyd, J, Pearce, C, Seidenkrantz, M-S. 2023. Distribution of modern benthic foraminiferal assemblages across the Northeast Greenland continental shelf. *Marine Micropaleontology* **184**: 102273. DOI: http://dx.doi.org/10.1016/j.marmicro.2023.102273.

Degen, R, Vedenin, A, Gusky, M, Boetius, A, Brey, T. 2015. Patterns and trends of macrobenthic abundance, biomass and production in the deep Arctic Ocean. *Polar Research* **34**(1): 24008. DOI: http://dx.doi.org/10.3402/polar.v34.24008.

Donis, D, McGinnis, DF, Holtappels, M, Felden, J, Wenzhoefer, F. 2016. Assessing benthic oxygen fluxes in oligotrophic deep sea sediments (HAUSGARTEN observatory). *Deep Sea Research Part I: Oceanographic Research Papers* **111**: 1–10.

Dybwad, C, Lalande, C, Bodur, YV, Henley, SF, Cottier, F, Ershova, EA, Hobbs, L, Last, KS, Dąbrowska, AM, Reigstad, M. 2022. The influence of sea ice cover and Atlantic Water advection on annual particle export north of Svalbard. *Journal of Geophysical Research: Oceans* **127**(10): e2022JC018897. DOI: http://dx.doi.org/10.1029/2022JC018897.

ENVEO. 2017. Greenland calving front dataset, 1990–2016, v2.0, Greenland Ice Sheet CCI. ENVEO. Available at http://cryoportal.enveo.at/data/. Accessed February 04, 2018.

Ezraty, R, Girard-Ardhuin, F, Piolle, J, Kaleschke, L, Heygster, G. 2007. *Arctic & Antarctic sea ice concentration and Arctic sea ice drift estimated from Special Sensor MIcrowave data—User's manual V2.1.* France: Departement d'Oceanographie Physique et Spatiale, IFREMER, Brest.

Falk-Petersen, S, Sargent, JR, Henderson, J, Hegseth, EN, Hop, H, Okolodkov, YB. 1998. Lipids and fatty acids in ice algae and phytoplankton from the Marginal Ice Zone in the Barents Sea. *Polar Biology* **20**:

41–47. DOI: http://dx.doi.org/10.1007/s00300 0050274.

Felden, J, **Wenzhöfer, F**, **Braeckman, U.** 2023. Ex situ diffusive oxygen uptake of the Northeast Greenland (NEG) shelf sediments from POLARSTERN cruise PS109. PANGAEA. DOI: https://doi.pangaea.de/10. 1594/PANGAEA.959545.

Gerlach, SA. 1971. On the importance of marine meiofauna for benthos communities. *Oecologia* **6**: 176–190. DOI: http://dx.doi.org/10.1007/BF00 345719.

Glud, RN, **Gundersen, JK**, **Barker Jørgensen, B**, **Revsbech, NP, Schulz, HD.** 1994. Diffusive and total oxygen uptake of deep-sea sediments in the eastern South Atlantic Ocean: *In situ* and laboratory measurements. *Deep Sea Research Part I: Oceanographic Research Papers* **41**(11–12): 1767–1788. DOI: http://dx.doi.org/10.1016/0967-0637(94)90072-8.

Górska, B, **Soltwedel, T**, **Schewe, I**, **Włodarska-Kowalczuk, M.** 2020. Bathymetric trends in biomass size spectra, carbon demand, and production of Arctic benthos (76–5561 m, Fram Strait). *Progress in Oceanography* **186**: 102370. DOI: http://dx.doi. org/10.1016/j.pocean.2020.102370.

Graf, G. 1989. Benthic-pelagic coupling in a deep-sea benthic community. *Nature* **341**: 437–439. DOI: http://dx.doi.org/10.1038/341437a0.

Graf, G, **Gerlach, SA**, **Linke, P**, **Queisser, W**, **Ritzrau, W**, **Scheltz, A**, **Thomsen, L**, **Witte, U.** 1995. Benthic-pelagic coupling in the Greenland-Norwegian Sea and its effect on the geological record. *Geologische Rundschau* **84**: 49–58. DOI: http://dx.doi.org/10. 1007/BF00192241.

Grebmeier, J, **McRoy, C**, **Feder, H.** 1988. Pelagic-benthic coupling on the shelf of the northern Bering and Chukchi Seas. I. Food supply source and benthic biomass. *Marine Ecology Progress Series* **48**: 57–67. DOI: http://dx.doi.org/10.3354/meps048057.

Grebmeier, J, **Overland, JE**, **Moore, SE**, **Farley, EV**, **Carmack, EC**, **Cooper, LW**, **Frey, KE**, **Helle, JH**, **McLaughlin, FA**, **McNutt, SL.** 2006. A major ecosystem shift in the Northern Bering Sea. *Science* **311**(5766): 1461–1464. DOI: http://dx.doi.org/10. 1126/science.1121365.

Grebmeier, JM, **Barry, JP.** 1991. The influence of oceanographic processes on pelagic-benthic coupling in polar regions: A benthic perspective. *Journal of Marine Systems* **2**(3–4): 495–518. DOI: http://dx. doi.org/10.1016/0924-7963(91)90049-Z.

Grebmeier, JM, **Barry, JP.** 2007. Benthic processes in polynyas, in Smith, WO, Barber, DG eds., *Elsevier oceanography series, polynyas: Windows to the world*: 363–390. DOI: http://dx.doi.org/10.1016/S0422-9894(06)74011-9.

Grebmeier, JM, **Bluhm, BA**, **Cooper, LW**, **Danielson, SL**, **Arrigo, KR**, **Blanchard, AL**, **Clarke, JT**, **Day, RH**, **Frey, KE**, **Gradinger, RR**, **Kędra, M**, **Konar, B**, **Kuletz, KJ**, **Lee, SH**, **Lovvorn, JR**, **Norcross, BL**, **Okkonen, SR.** 2015. Ecosystem characteristics and processes facilitating persistent macrobenthic biomass hotspots and associated benthivory in the Pacific Arctic. *Progress in Oceanography* **136**: 92–114. DOI: http://dx.doi.org/10.1016/j.pocean. 2015.05.006.

Gutt, J. 1995. The occurrence of sub-ice algal aggregations off northeast Greenland. *Polar Biology* **15**: 247–252. DOI: http://dx.doi.org/10.1007/BF00239844.

Hegseth, EN. 1998. Primary production of the northern Barents Sea. *Polar Research* **17**: 113–123. Available at https://onlinelibrary.wiley.com/doi/abs/10. 1111/j.1751-8369.1998.tb00266.x.

Heip, C, **Vincx, M**, **Vranken, G.** 1985. The ecology of marine nematodes, in Barnes, H, Barnes, M eds., *Oceanography and marine biology, an annual review.* Aberdeen, UK: Aberdeen University Press: 399–489.

Hobbie, JE, **Daley, RJ**, **Jasper, S.** 1977. Use of nuclepore filters for counting bacteria by fluorescence microscopy. *Applied and Environmental Microbiology* **33**: 1225–1228.

Hobson, KA, **Ambrose, WG**, **Renaud, PR.** 1995. Sources of primary production, benthic-pelagic coupling, and trophic relationships within the northeast Water Polynya: Insights from ∂13C and ∂15N analysis. *Marine Ecology Progress Series* **128**: 1–10.

Hoffmann, R, **Braeckman, U**, **Hasemann, C**, **Wenzhöfer, F.** 2018. Deep-sea benthic communities and oxygen fluxes in the Arctic Fram Strait controlled by sea-ice cover and water depth. *Biogeosciences* **15**: 1–40. DOI: http://dx.doi.org/10.5194/bg-2017-537.

Horner, R, **Schrader, GC.** 1982. Relative contributions of ice algae, phytoplankton, and benthic microalgae to primary production in nearshore regions of the Beaufort Sea. *Arctic* **35**(4): 485–503. DOI: http:// dx.doi.org/10.14430/arctic2356.

Hughes, NE, **Wilkinson, JP**, **Wadhams, P.** 2011. Multi-satellite sensor analysis of fast-ice development in the Norske Øer Ice Barrier, Northeast Greenland. *Annals of Glaciology* **52**: 151–160. DOI: http://dx. doi.org/10.3189/172756411795931633.

Ingels, J, **Van den Driessche, P**, **De Mesel, I**, **Vanhove, S**, **Moens, T**, **Vanreusel, A.** 2010. Preferred use of bacteria over phytoplankton by deep-sea nematodes in polar regions. *Marine Ecology Progress Series* **406**: 121–133. DOI: http://dx.doi.org/10. 3354/meps08535.

International Space Science Institute. 2008. Arctic change and polynyas: Focus on the Northeast Water Polynya and North Water Polynya/Nares Strait system team. Available at http://www.issibern.ch/ teams/Polynya/. Accessed November 2, 2018.

Jakobsson, M, **Mayer, LA**, **Bringensparr, C**, **Castro, CF**, **Mohammad, R**, **Johnson, P**, **Ketter, T**, **Accettella, D**, **Amblas, D**, **An, L**, **Arndt, JE**, **Canals, M**, **Casamor, JL**, **Chauché, N**, **Coakley, B**, **Danielson, S**, **Demarte, M**, **Dickson, M-L**, **Dorschel, B**, **Dowdeswell, JA**, **Dreutter, S**, **Fremand, AC**, **Gallant, D**, **Hall, JK**, **Hehemann, L**, **Hodnesdal, H**, **Hong, J**, **Ivaldi, R**, **Kane, E**, **Klaucke, I**, **Krawczyk, DW**, **Kristoffersen, Y**, **Kuipers, BR**, **Millan, R**, **Masetti, G**, **Morlighem, M**, **Noormets, R**, **Prescott, MM**,

Rebesco, M, Rignot, E, Semiletov, I, Tate, AJ, Travaglini, P, Velicogna, I, Weatherall, P, Weinrebe, W, Willis, JK, Wood, M, Zarayskaya, Y, Zhang, T, Zimmermann, M, Zinglersen, KB. 2020. The International Bathymetric Chart of the Arctic Ocean version 4.0. *Scientific Data* **7**(1): 176. DOI: http://dx.doi.org/10.1038/s41597-020-0520-9.

Jensen, M, Lomstein, E, Sørensen, J. 1990. Benthic NH_4^+ and NO_3^- flux following sedimentation of a spring phytoplankton bloom in Aarhus Bight, Denmark. *Marine Ecology Progress Series* **61**: 87–96. DOI: http://dx.doi.org/10.3354/meps061087.

Kaleschke, L, Lüpkes, C, Vihma, T, Haarpaintner, J, Bochert, A, Hartmann, J, Heygster, G. 2001. SSM/I sea ice remote sensing for mesoscale ocean-atmosphere interaction analysis. *Canadian Journal of Remote Sensing* **27**(5): 526–537. DOI: http://dx.doi.org/10.1080/07038992.2001.10854892.

Kanzow, T, Rohardt, G. 2017. CTD raw data files from POLARSTERN cruise PS109, link to tar-archive. PANGAEA. DOI: http://dx.doi.org/10.1594/PANGAEA.883366.

Kanzow, T, Schaffer, J, Rohardt, G. 2018. Physical oceanography during POLARSTERN cruise PS109 (ARK-XXXI/4). PANGAEA. DOI: http://dx.doi.org/10.1594/PANGAEA.885358.

Kędra, M, Kuliński, K, Walkusz, W, Legeżyńska, J. 2012. The shallow benthic food web structure in the high Arctic does not follow seasonal changes in the surrounding environment. *Estuarine, Coastal and Shelf Science* **114**: 183–191. DOI: http://dx.doi.org/10.1016/j.ecss.2012.08.015.

Khan, SA, Kjær, KH, Bevis, M, Bamber, JL, Wahr, J, Kjeldsen, KK, Bjørk, AA, Korsgaard, NJ, Stearns, LA, van den Broeke, MR, Liu, L, Larsen, NK, Muresan, IS. 2014. Sustained mass loss of the northeast Greenland ice sheet triggered by regional warming. *Nature Climate Change* **4**: 292–299. DOI: http://dx.doi.org/10.1038/nclimate2161.

Li, WKW, McLaughlin, FA, Lovejoy, C, Carmack, EC. 2009. Smallest algae thrive as the Arctic Ocean freshens. *Science* **326**(5952): 539. DOI: http://dx.doi.org/10.1126/science.1179798.

Mäkelä, A, Witte, U, Archambault, P. 2017. Ice algae versus phytoplankton: Resource utilization by Arctic deep sea macroinfauna revealed through isotope labelling experiments. *Marine Ecology Progress Series* **572**: 1–18. DOI: http://dx.doi.org/10.3354/meps12157.

Mayer, C, Reeh, N, Jung-Rothenhäusler, F, Huybrechts, P, Oerter, H. 2000. The subglacial cavity and implied dynamics under Nioghalvfjerdsfjorden Glacier, NE-Greenland. *Geophysical Research Letters* **27**(15): 2289–2292. DOI: http://dx.doi.org/10.1029/2000GL011514.

Mayer, C, Schaffer, J, Hattermann, T, Floricioiu, D, Krieger, L, Dodd, PA, Kanzow, T, Licciulli, C, Schannwell, C. 2018. Large ice loss variability at Nioghalvfjerdsfjorden Glacier, Northeast-Greenland. *Nature Communications* **9**: 2768. DOI: http://dx.doi.org/10.1038/s41467-018-05180-x.

McMahon, K, Ambrose, WG, Johnson, B, Sun, M, Lopez, G, Clough, L, Carroll, M. 2006. Benthic community response to ice algae and phytoplankton in Ny Ålesund, Svalbard. *Marine Ecology Progress Series* **310**: 1–14. DOI: http://dx.doi.org/10.3354/meps310001.

McTigue, ND, Bucolo, P, Liu, Z, Dunton, KH. 2015. Pelagic-benthic coupling, food webs, and organic matter degradation in the Chukchi Sea: Insights from sedimentary pigments and stable carbon isotopes. *Limnology and Oceanography* **60**: 429–445. DOI: http://dx.doi.org/10.1002/lno.10038.

Meire, L, Mortensen, J, Rysgaard, S, Bendtsen, J, Boone, W, Meire, P, Meysman, FJR. 2016. Spring bloom dynamics in a subarctic fjord influenced by tidewater outlet glaciers (Godthåbsfjord, SW Greenland): Spring in a subarctic fjord. *Journal of Geophysical Research: Biogeosciences* **121**(6): 1581–1592. DOI: http://dx.doi.org/10.1002/2015JG003240.

Meredith, M, Sommerkorn, M, Cassota, S, Derksen, C, Ekaykin, A, Hollowed, A, Kofinas, G, Mackintosh, A, Melbourne-Thomas, J, Muelbert, MMC, Ottersen, G, Pritchard, H, Schuur, EAG. 2019. Polar regions, in Pörtner, HO, Roberts, DC, Masson-Delmotte, V, Zhai, P, Tignor, M, Poloczanska, ES, Mintenbeck, K, Alegría, A, Nicolai, M, Okem, A, Petzold, J, Rama, B, Weyer, NM eds., *IPCC special report on the ocean and cryosphere in a changing climate*. Cambridge University Press: 203–320. DOI: http://dx.doi.org/10.1017/9781009157964.

Minnett, PJ, Bignami, F, Böhm, E, Budéus, G, Galbraith, PS, Gudmandsen, P, Hopkins, TS, Ingram, RG, Johnson, MA, Niebauer, HJ, Ramseier, RO, Schneider, W. 1997. A summary of the formation and seasonal progression of the Northeast Water Polynya. *Journal of Marine Systems* **10**(1–4): 79–85. DOI: http://dx.doi.org/10.1016/S0924-7963(96)00060-7.

Morata, N, Michaud, E, Włodarska-Kowalczuk, M. 2015. Impact of early food input on the Arctic benthos activities during the polar night. *Polar Biology* **38**: 99–114. DOI: http://dx.doi.org/10.1007/s00300-013-1414-5.

Morata, N, Renaud, PE. 2008. Sedimentary pigments in the western Barents Sea: A reflection of pelagic–benthic coupling? *Deep Sea Research Part II: Topical Studies in Oceanography* **55**(20–21): 2381–2389. DOI: http://dx.doi.org/10.1016/j.dsr2.2008.05.004.

Nemys eds. 2022. Nemys: World database of nematodes. DOI: http://dx.doi.org/10.14284/366.

Nick, FM, Vieli, A, Andersen, ML, Joughin, I, Payne, A, Edwards, TL, Pattyn, F, van de Wal, RSW. 2013. Future sea-level rise from Greenland's main outlet glaciers in a warming climate. *Nature* **497**: 235–238. DOI: http://dx.doi.org/10.1038/nature12068.

Niebauer, HJ, Alexander, V, Henrichs, S. 1990. Physical and biological oceanographic interaction in the

spring bloom at the Bering Sea marginal ice edge zone. *Journal of Geophysical Research: Oceans* **95**(C12): 22229–22241. DOI: http://dx.doi.org/10.1029/JC095iC12p22229.

Oksanen, J, Blanchet, FG, Friendly, M, Kindt, R, Legendre, P, McGlinn, D, Minchin, PR, O'Hara, RB, Simpson, GL, Solymos, P, Stevens, MHH, Szoecs, E, Wagner, H. 2018. Vegan: Community ecology package, version 2.5. Available at https://CRAN.R-project.org/package=vegan. Accessed August 22, 2018.

Olli, K, Wassmann, P, Reigstad, M, Ratkova, TN, Arashkevich, E, Pasternak, A, Matrai, P, Knulst, J, Tranvik, L, Klais, R, Jacobsen, A. 2007. The fate of production in the central Arctic Ocean—Top-down regulation by zooplankton expatriates? *Progress in Oceanography* **72**(1): 84–113. DOI: http://dx.doi.org/10.1016/j.pocean.2006.08.002.

Onarheim, IH, Eldevik, T, Smedsrud, LH, Stroeve, JC. 2018. Seasonal and regional manifestation of Arctic Sea ice loss. *Journal of Climate* **31**(12): 4917–4932. DOI: http://dx.doi.org/10.1175/JCLI-D-17-0427.1.

Overland, JE, Wang, M. 2013. When will the summer Arctic be nearly sea ice free? *Geophysical Research Letters* **40**(10): 2097–2101. DOI: http://dx.doi.org/10.1002/grl.50316.

Pabi, S, van Dijken, GL, Arrigo, KR. 2008. Primary production in the Arctic Ocean, 1998–2006. *Journal of Geophysical Research: Oceans* **113**: C8. DOI: http://dx.doi.org/10.1029/2007JC004578.

Pesant, S, Legendre, L, Gosselin, M, Bjornsen, PK, Fortier, L, Michaud, J, Nielsen, TG. 2000. Pathways of carbon cycling in marine surface waters: The fate of small-sized phytoplankton in the Northeast Water Polynya. *Journal of Plankton Research* **22**(4): 779–801. DOI: http://dx.doi.org/10.1093/plankt/22.4.779.

Pesant, S, Legendre, L, Gosselin, M, Smith, R, Kattner, G, Ramseier, R. 1996. Size-differential regimes of phytoplankton production in the Northeast Water Polynya (77°–81°N). *Marine Ecology Progress Series* **142**: 75–86. DOI: http://dx.doi.org/10.3354/meps142075.

Piepenburg, D. 2005. Recent research on Arctic benthos: Common notions need to be revised. *Polar Biology* **28**(10): 733–755. DOI: http://dx.doi.org/10.1007/s00300-005-0013-5.

Piepenburg, D, Ambrose, WG, Brandt, A, Renaud, PE, Ahrens, MJ, Jensen, P. 1997. Benthic community patterns reflect water column processes in the Northeast Water polynya (Greenland). *Journal of Marine Systems* **10**(1–4): 467–482. DOI: http://dx.doi.org/10.1016/S0924-7963(96)00050-4.

Piepenburg, D, Archambault, P, Ambrose, WG, Blanchard, AL, Bluhm, BA, Carroll, ML, Conlan, KE, Cusson, M, Feder, HM, Grebmeier, JM, Jewett, SC, Lévesque, M, Petryashev, VV, Sejr, MK, Sirenko, BI, Włodarska-Kowalczuk, M. 2011. Towards a pan-Arctic inventory of the species diversity of the macro- and megabenthic fauna of the Arctic shelf seas. *Marine Biodiversity* **41**: 51–70. DOI: http://dx.doi.org/10.1007/s12526-010-0059-7.

Piepenburg, D, Blackburn, T, von Dorrien, C, Gutt, J, Hall, P, Hulth, S, Kendall, M, Opalinski, K, Rachor, E, Schmid, M. 1995. Partitioning of benthic community respiration in the Arctic (northwestern Barents Sea). *Marine Ecology Progress Series* **118**: 199–213. DOI: http://dx.doi.org/10.3354/meps118199.

Polyakov, IV, Alkire, MB, Bluhm, BA, Brown, KA, Carmack, EC, Chierici, M, Danielson, SL, Ellingsen, I, Ershova, EA, Gårdfeldt, K, Ingvaldsen, RB, Pnyushkov, AV, Slagstad, D, Wassmann, P. 2020. Borealization of the Arctic Ocean in response to anomalous advection from sub-Arctic seas. *Frontiers in Marine Science* **7**: 491. DOI: http://dx.doi.org/10.3389/fmars.2020.00491.

Preben, J, Herman, R. 2023. Abundance of nematoda genera on the Northeast Greenland shelf collected between May and August 1993 with USCG Polar Sea and R/V Polarstern (ARK VIII/2). PANGAEA. DOI: http://dx.doi.org/10.1594/PANGAEA.959509.

R Core Team. 2018. R: A language and environment for statistical computing. Vienna, Austria: R Foundation for Statistical Computing. Available at https://www.R-project.org/. Accessed August 20, 2018.

Reeh, N. 2017. Greenland ice shelves and ice tongues, in Copland, L, Mueller, D eds., *Arctic ice shelves and ice islands*. Springer: 75–106. DOI: http://dx.doi.org/10.1007/978-94-024-1101-0.

Reeh, N, Thomsen, HH, Higgins, AK, Weidick, A. 2001. Sea ice and the stability of north and northeast Greenland floating glaciers. *Annals of Glaciology* **33**: 474–480. DOI: http://dx.doi.org/10.3189/172756401781818554.

Renaud, PE, Ambrose, WGJ. 2023. Benthic polychaeta diversity on the Northeast Greenland (NEG) shelf collected between July–August 1992 and between May and August 1993. DOI: http://dx.doi.org/10.1594/PANGAEA.959541.

Renaud, PE, Morata, N, Carroll, ML, Denisenko, SG, Reigstad, M. 2008. Pelagic–benthic coupling in the western Barents Sea: Processes and time scales. *Deep Sea Research Part II: Topical Studies in Oceanography* **55**(20–21): 2372–2380. DOI: http://dx.doi.org/10.1016/j.dsr2.2008.05.017.

Renaud, PE, Riedel, A, Michel, C, Morata, N, Gosselin, M, Juul-Pedersen, T, Chiuchiolo, A. 2007. Seasonal variation in benthic community oxygen demand: A response to an ice algal bloom in the Beaufort Sea, Canadian Arctic? *Journal of Marine Systems* **67**: 1–12. DOI: http://dx.doi.org/10.1016/j.jmarsys.2006.07.006.

Revsbech, NP. 1989. An oxygen microsensor with a guard cathode. *Limnology and Oceanography* **34**(2): 474–478. DOI: http://dx.doi.org/10.4319/lo.1989.34.2.0474.

Rignot, E, Kanagaratnam, P. 2006. Changes in the velocity structure of the Greenland ice sheet. *Science* **311**:

986–990. DOI: http://dx.doi.org/10.1126/science. 1121381.

Rowe, GT, Boland, GS, Escobar-Briones, EG, Cruz-Kaegi, ME, Newton, A, Piepenburg, D, Walsh, I, Deming, J. 1997. Sediment community biomass and respiration in the Northeast water polynya, Greenland: A numerical simulation of benthic lander and spade core data. *Journal of Marine Systems* 10: 497–515. DOI: http://dx.doi.org/10.1016/S0924-7963(96)00065-6.

Sakshaug, E, Johnsen, G, Kristiansen, S, von Quillfeldt, CH, Rey, F, Slagstad, D, Thingstad, F. 2009. Phytoplankton and primary production, in Sakshaug, E, Johnsen, G, Kovacs, KM eds., *Ecosystem Barents Sea*. Trondheim, Norway: Tapir Academic Press: 167–208.

Sakshaug, E, Skjoldal, HR. 1989. Life at the ice edge. *Ambio* 18: 60–67.

Schaffer, J, Kanzow, T, von Appen, W-J, Albedyll, L, von Arndt, JE, Roberts, DH. 2020. Bathymetry constrains ocean heat supply to Greenland's largest glacier tongue. *Nature Geoscience* 13: 227–231. DOI: http://dx.doi.org/10.1038/s41561-019-0529-x.

Schaffer, J, von Appen, W-J, Dodd, PA, Hofstede, C, Mayer, C, de Steur, L, Kanzow, T. 2017. Warm water pathways toward Nioghalvfjerdsfjorden Glacier, Northeast Greenland. *Journal of Geophysical Research: Oceans* 122(5): 4004–4020. DOI: http://dx.doi.org/10.1002/2016JC012462.

Schneider, W, Budéus, G. 1994. The Northeast Water Polynya (Greenland Sea) I. A physical concept of its generation. *Polar Biology* 14: 1–9.

Seinhorst, JW. 1959. A rapid method for the transfer of nematodes from fixative to anhydrous glycerin. *Nematologica* 4: 67–69.

Sejr, MK, Jensen, KT, Rysgaard, S. 2000. Macrozoobenthic community structure in a high-Arctic East Greenland fjord. *Polar Biology* 23: 792–801. DOI: http://dx.doi.org/10.1007/s003000000154.

Sejr, MK, Stedmon, CA, Bendtsen, J, Abermann, J, Juul-Pedersen, T, Mortensen, J, Rysgaard, S. 2017. Evidence of local and regional freshening of Northeast Greenland coastal waters. *Scientific Reports* 7: 13183. DOI: http://dx.doi.org/10.1038/s41598-017-10610-9.

Skagseth, Ø, Eldevik, T, Årthun, M, Asbjørnsen, H, Lien, VS, Smedsrud, LH. 2020. Reduced efficiency of the Barents Sea cooling machine. *Nature Climate Change* 10: 661–666. DOI: http://dx.doi.org/10.1038/s41558-020-0772-6.

Smedsrud, LH, Muilwijk, M, Brakstad, A, Madonna, E, Lauvset, SK, Spensberger, C, Born, A, Eldevik, T, Drange, H, Jeansson, E, Li, C, Olsen, A, Skagseth, Ø, Slater, DA, Straneo, F, Våge, K, Årthun, M. 2022. Nordic seas heat loss, Atlantic inflow, and Arctic sea ice cover over the last century. *Reviews of Geophysics* 60(1): e2020RG000725. DOI: http://dx.doi.org/10.1029/2020RG000725.

Smith, KL, Ruhl, HA, Kahru, M, Huffard, CL, Sherman, AD. 2013. Deep ocean communities impacted by changing climate over 24 y in the abyssal northeast Pacific Ocean. *Proceedings of the National Academy of Sciences* 110(49): 19838–19841. DOI: http://dx.doi.org/10.1073/pnas.1315447110.

Smith, WO, Barber, DG. 2007. Polynyas and climate change: A view to the future, in Smith, WO, Barber, DG eds., *Elsevier oceanography series, polynyas: Windows to the world*. Elsevier: 74: 411–419. DOI: http://dx.doi.org/10.1016/S0422-9894(06) 74013-2.

Spielhagen, RF, Werner, K, Sørensen, SA, Zamelczyk, K, Kandiano, E, Budeus, G, Husum, K, Marchitto, TM, Hald, M. 2011. Enhanced modern heat transfer to the Arctic by warm Atlantic Water. *Science* 331(6016): 450–453. DOI: http://dx.doi.org/10.1126/science.1197397.

Spies, A. 1987. Phytoplankton in the Marginal Ice Zone of the Greenland Sea during summer, 1984. *Polar Biology* 7: 195–205. DOI: http://dx.doi.org/10.1007/BF00287416.

Spreen, G, de Steur, L, Divine, D, Gerland, S, Hansen, E, Kwok, R. 2020. Arctic sea ice volume export through Fram Strait from 1992 to 2014. *Journal of Geophysical Research: Oceans* 125(6): e2019JC016039. DOI: http://dx.doi.org/10.1029/2019JC016039.

Stirling, I. 1997. The importance of polynyas, ice edges, and leads to marine mammals and birds. *Journal of Marine Systems* 10(1–4): 9–21. DOI: http://dx.doi.org/10.1016/S0924-7963(96)00054-1.

Straneo, F, Sutherland, DA, Holland, DM, Gladish, C, Hamilton, GS, Johnson, HL, Rignot, E, Xu, Y, Koppes, M. 2012. Characteristics of ocean waters reaching Greenland's glaciers. *Annals of Glaciology* 53(60): 202–210. DOI: http://dx.doi.org/10.3189/2012AoG60A059.

Stroeve, JC, Serreze, MC, Holland, MM, Kay, JE, Malanik, J, Barrett, AP. 2012. The Arctic's rapidly shrinking sea ice cover: A research synthesis. *Climatic Change* 110: 1005–1027. DOI: http://dx.doi.org/10.1007/s10584-011-0101-1.

Sumata, H, de Steur, L, Gerland, S, Divine, DV, Pavlova, O. 2022. Unprecedented decline of Arctic Sea ice outflow in 2018. *Nature Communications* 13: 1747. DOI: http://dx.doi.org/10.1038/s41467-022-29470-7.

Syring, N, Stein, R, Fahl, K, Vahlenkamp, M, Zehnich, M, Spielhagen, RF, Niessen, F. 2020. Holocene changes in sea-ice cover and polynya formation along the eastern North Greenland shelf: New insights from biomarker records. *Quaternary Science Reviews* 231: 106173. DOI: http://dx.doi.org/10.1016/j.quascirev.2020.106173.

Tengberg, A, De Bovee, F, Hall, P, Berelson, W, Chadwick, D, Ciceri, G, Crassous, P, Devol, A, Emerson, S, Gage, J. 1995. Benthic chamber and profiling landers in oceanography—A review of design, technical solutions and functioning. *Progress in Oceanography* 35(3): 253–294.

Thomsen, HH, **Reeh, N**, **Olesen, OB**, **Boggild, CE**, **Starzer, W**, **Weidick, A**, **Higgins, AK.** 1997. The Nioghalvfjerdsfjorden glacier project, North-East Greenland: A study of ice sheet response to climatic change. *Geology of Greenland Survey Bulletin* **176**: 95–103.

Veit-Köhler, G, **Durst, S**, **Schuckenbrock, J**, **Hauquier, F**, **Durán Suja, L**, **Dorschel, B**, **Vanreusel, A**, **Martínez Arbizu, P.** 2018. Oceanographic and topographic conditions structure benthic meiofauna communities in the Weddell sea, Bransfield Strait and Drake Passage (Antarctic). *Progress in Oceanography* **162**: 240–256. DOI: http://dx.doi.org/10.1016/j.pocean.2018.03.005.

von Appen, W-J, **Waite, AM**, **Bergmann, M**, **Bienhold, C**, **Boebel, O**, **Bracher, A**, **Cisewski, B**, **Hagemann, J**, **Hoppema, M**, **Iversen, MH**, **Konrad, C**, **Krumpen, T**, **Lochthofen, N**, **Metfies, K**, **Niehoff, B**, **Nöthig, E-M**, **Purser, A**, **Salter, I**, **Schaber, M**, **Scholz, D**, **Soltwedel, T**, **Torres-Valdes, S**, **Wekerle, C**, **Wenzhöfer, F**, **Wietz, M**, **Boetius, A**. 2021. Sea-ice derived meltwater stratification slows the biological carbon pump: Results from continuous observations. *Nature Communications* **12**: 7309. DOI: http://dx.doi.org/10.1038/s41467-021-26943-z.

Wadhams, P. 1981. The ice cover in the Greenland and Norwegian seas. *Reviews of Geophysics* **19**(3): 345–393. DOI: http://dx.doi.org/10.1029/RG019i003p00345.

Wassmann, P, **Reigstad, M.** 2011. Future Arctic Ocean seasonal ice zones and implications for pelagic-benthic coupling. *Oceanography* **24**(3): 220–231. DOI: http://dx.doi.org/10.5670/oceanog.2011.74.

Wessel, P, **Smith, WHF.** 1996. A global, self-consistent, hierarchical, high-resolution shoreline database. *Journal of Geophysical Research: Solid Earth* **101**(B4): 8741–8743. DOI: http://dx.doi.org/10.1029/96JB00104.

Whitaker, D. 2021. Clustsig. Available at https://github.com/douglaswhitaker/clustsig. Accessed November 9, 2022.

Wiedmann, I, **Ershova, E**, **Bluhm, BA**, **Nöthig, EM**, **Gradinger, RR**, **Kosobokova, K**, **Boetius, A.** 2020. What feeds the benthos in the Arctic basins? Assembling a carbon budget for the deep Arctic Ocean. *Frontiers in Marine Science* **7**: 224. DOI: http://dx.doi.org/10.3389/fmars.2020.00224.

Wieser, W. 1953. Die Beziehung zwischen Mundhöhlengestalt, Ernährungsweise und Vorkommen bei freilebenden marinen Nematoden: Eine ökologisch-morphologische studie. *Arkiv för zoologi* **2**(Ser 4): 439–484.

Wilson, NJ, **Straneo, F.** 2015. Water exchange between the continental shelf and the cavity beneath Nioghalvfjerdsbræ (79 North Glacier). *Geophysical Research Letters* **42**(18): 7648–7654. DOI: http://dx.doi.org/10.1002/2015GL064944.

Włodarska-Kowalczuk, M, **Górska, B**, **Deja, K**, **Morata, N.** 2016. Do benthic meiofaunal and macrofaunal communities respond to seasonality in pelagial processes in an Arctic fjord (Kongsfjorden, Spitsbergen)? *Polar Biology* **39**: 2115–2129. DOI: http://dx.doi.org/10.1007/s00300-016-1982-2.

Włodarska-Kowalczuk, M, **Pearson, TH.** 2004. Soft-bottom macrobenthic faunal associations and factors affecting species distributions in an Arctic glacial fjord (Kongsfjord, Spitsbergen). *Polar Biology* **27**: 155–167. DOI: http://dx.doi.org/10.1007/s00300-003-0568-y.

Włodarska-Kowalczuk, M, **Pearson, TH**, **Kendall, MA.** 2005. Benthic response to chronic natural physical disturbance by glacial sedimentation in an Arctic fjord. *Marine Ecology Progress Series* **303**: 31–41. DOI: http://dx.doi.org/10.3354/meps303031.

Włodarska-Kowalczuk, M, **Renaud, PE**, **Węsławski, JM**, **Cochrane, SK**, **Denisenko, SG.** 2012. Species diversity, functional complexity and rarity in Arctic fjordic versus open shelf benthic systems. *Marine Ecology Progress Series* **463**: 73–87. DOI: http://dx.doi.org/10.3354/meps09858.

Wright, SW, **Jeffrey, SW.** 1997. High-resolution HPLC system for chlorophylls and carotenoids of marine phytoplankton, in Jeffrey, SW, Wright, SW, Mantoura, RFC eds., *Phytoplankton pigments in oceanography: Guidelines to modern methods*. Paris, France: UNESCO Pub.

ELEMENTA
Science of the Anthropocene

Elem Sci Anth is a peer-reviewed open access journal published by University of California Press.

OPEN ACCESS